# Advanced Thermal Solutions for Emerging High-Density Electronic Systems

Dr Evgeny Zamburg, Dr Yizhou Jiang, Dr Baochang Xu, Dr Gan Zhang

PI: Prof Aaron Voon-Yew Thean

Singapore Hybrid-Integrated Next-Generation μ-Electronics (SHINE) Centre
Department of Electrical and Computer Engineering, National University of Singapore

EU – Singapore Workshop on Semiconductors
9 July 2025

# AI and high-frequency RF applications drives power density increase

# Outline

- Wafer-level thermal management during chip fabrication
  - Thermoelectric solution
  - Micro-jet solution
- Interposer-Level Thermal Management
  - SiC vs Si
- PCB-Level Thermal Management
  - Passive heat spreading with Ga/PCM composites
  - Active Cooling with Magnetic PCM Slurry

# Overview of Cooling Techniques

## Active

Requires Moving Parts

Fan → Air

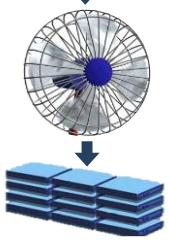

Mechanical Pump → Liquid

## Passive

Constrained by Material Properties

Phase-changing Materials (PCM)

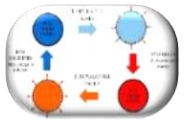

Heat Sink

Heat Pipe

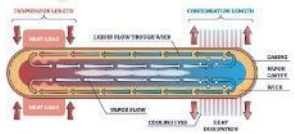

Pure PCM

Composite

PCM with Carbon-based

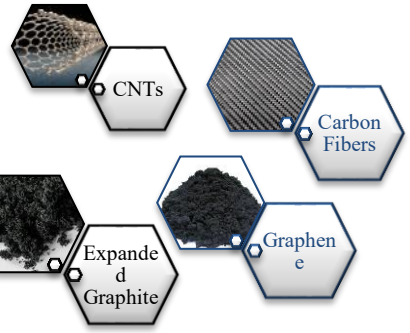


PCM with Metal-based

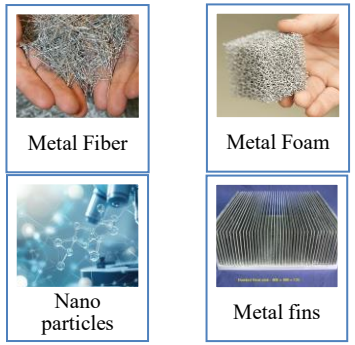


## Hybrid

Go beyond Machinery and Materials

PCM + Air Cooling

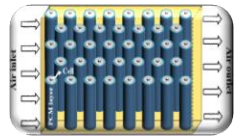

PCM + Heat Pipe

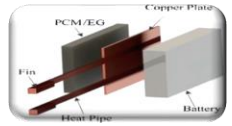


PCM + Liquid Cooling

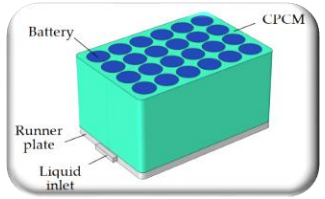


Enhanced heat Absorption with PCM
Forced Convection by fluid motion

# Wafer-Level Thermal Management During Chip Fabrication

# Thermal Challenges in Wafer-Level Testing

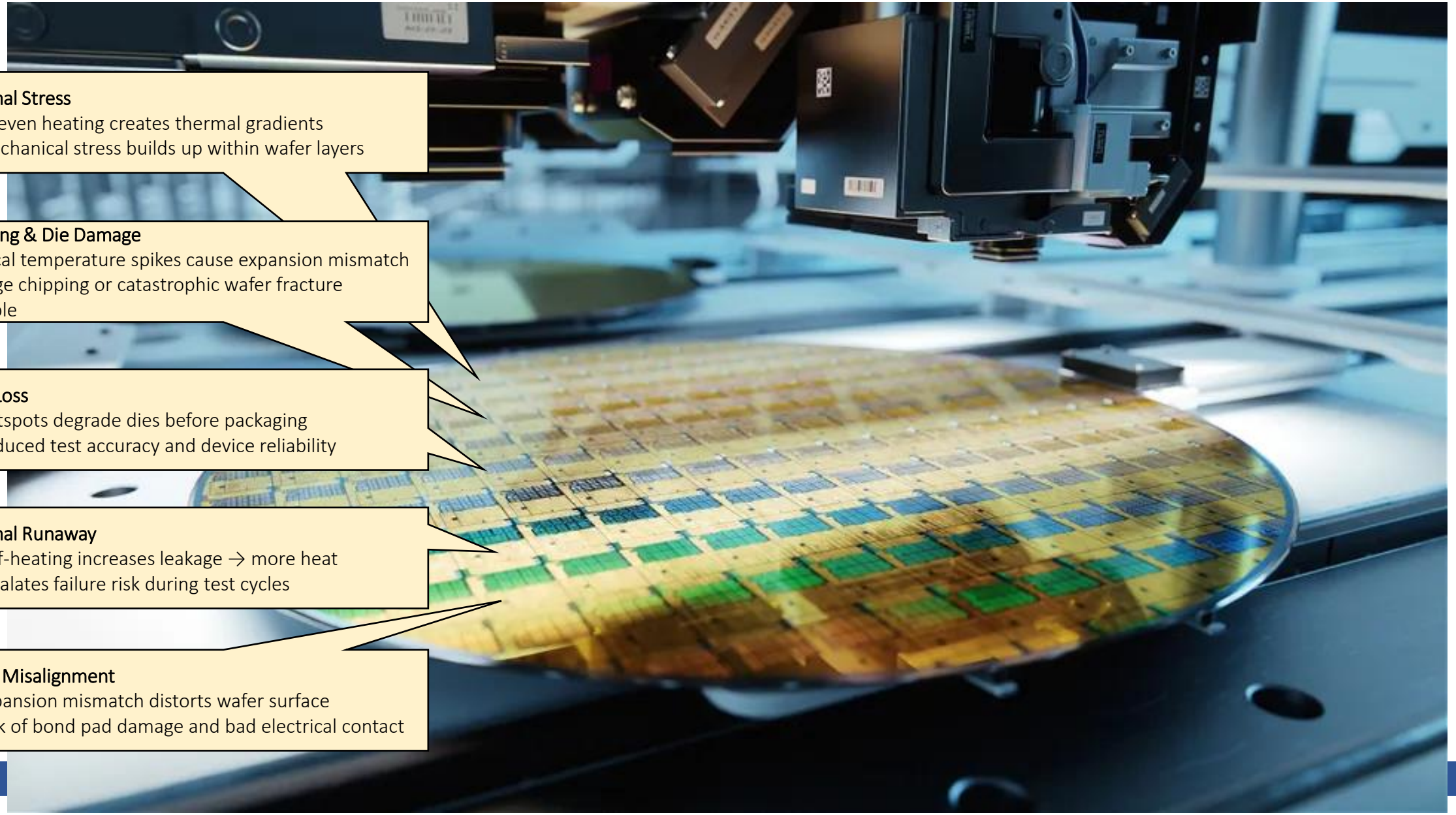

**Thermal Stress**
→ Uneven heating creates thermal gradients
→ Mechanical stress builds up within wafer layers

**Cracking & Die Damage**
→ Local temperature spikes cause expansion mismatch
→ Edge chipping or catastrophic wafer fracture possible

**Yield Loss**
→ Hotspots degrade dies before packaging
→ Reduced test accuracy and device reliability

**Thermal Runaway**
→ Self-heating increases leakage → more heat
→ Escalates failure risk during test cycles

**Probe Misalignment**
→ Expansion mismatch distorts wafer surface
→ Risk of bond pad damage and bad electrical contact

# Prototype of Wafer-Level Thermal Management System

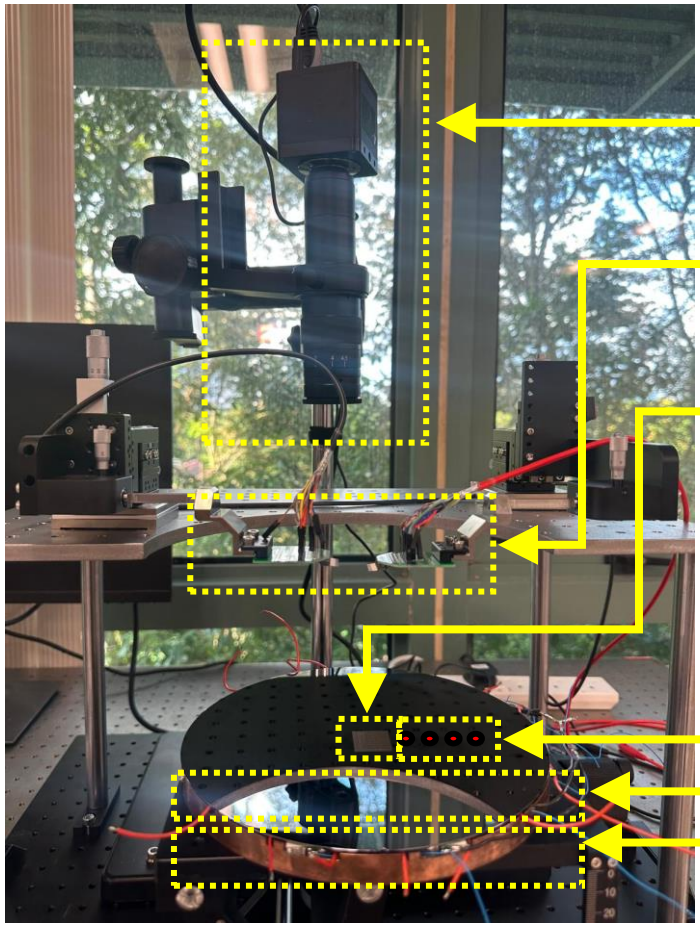

- Microscope
- Probe cards
- **Thermal test chip**
- Thermocouples
- 8-inch wafer
- **TEC cooling chuck**

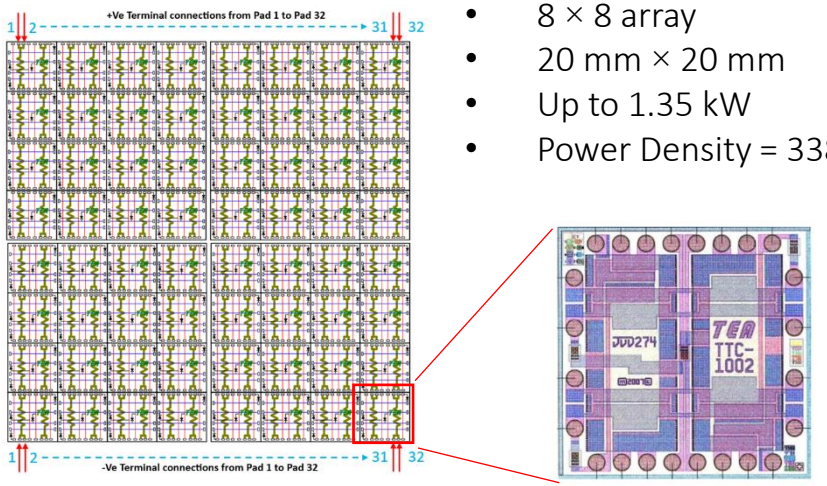


- 8 × 8 array
- 20 mm × 20 mm
- Up to 1.35 kW
- Power Density = 338 W/cm$^2$

Thermal test chip array for high power and controllable heat generation during testing

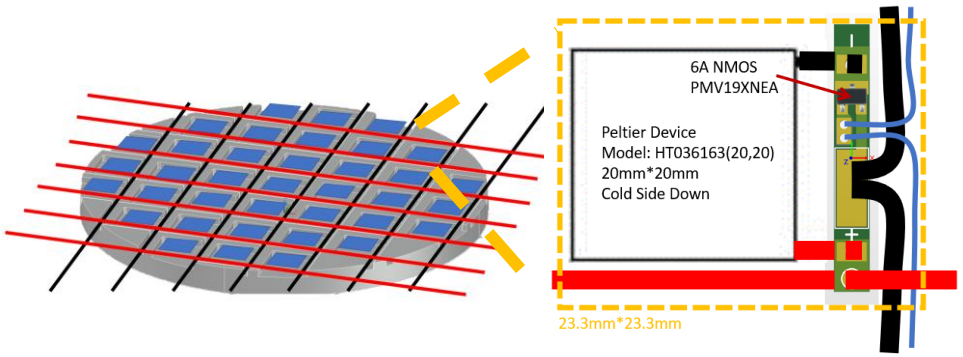


Designed testing rig with commercial TE device for high power thermal management system during wafer-scale testing

# Thermoelectric Array Approach

# Liquid Cooling Vs Hybrid Thermoelectric Cooling

**Liquid cooling:**

- Purely rely on cooling liquid below substrate.

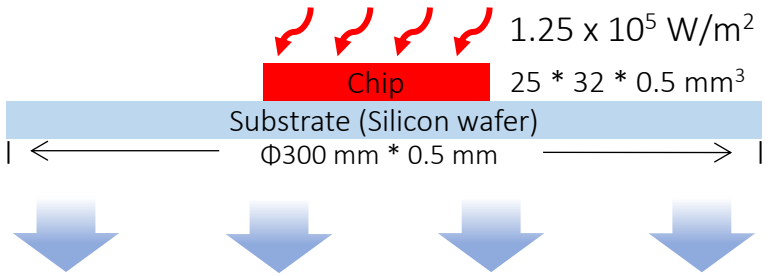


$T_{liquid}$ = 233.15 K, $h$ = 1 x $10^3$ W/$m^2$-K

**Hybrid cooling:**

- Chip is cooled down by TE cooler embedded in copper heat sink.
- The hot side of TE cooler is cooled down by cooling liquid.

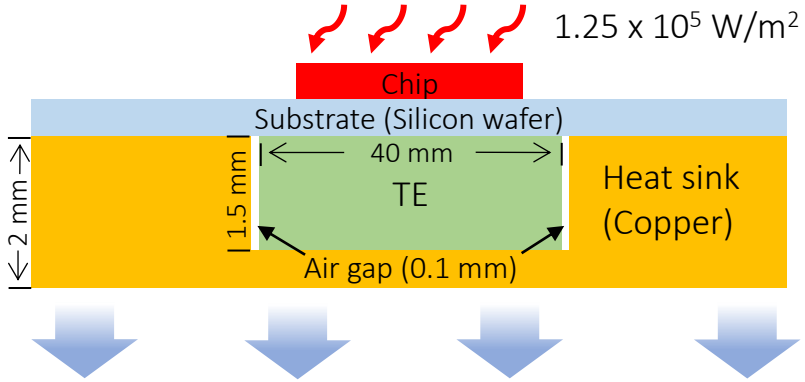


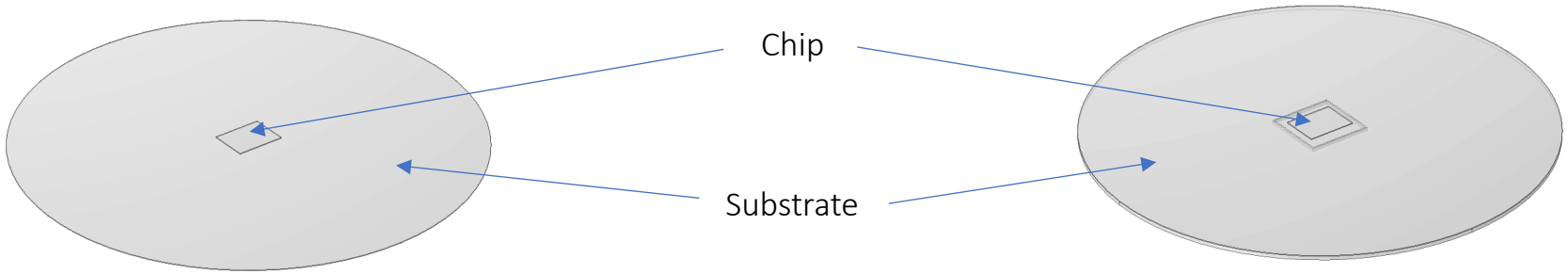

# Thermal Performance of Thermoelectric Cooling

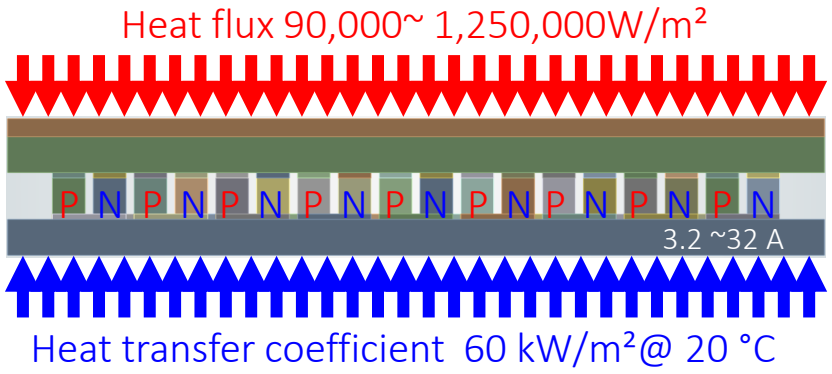


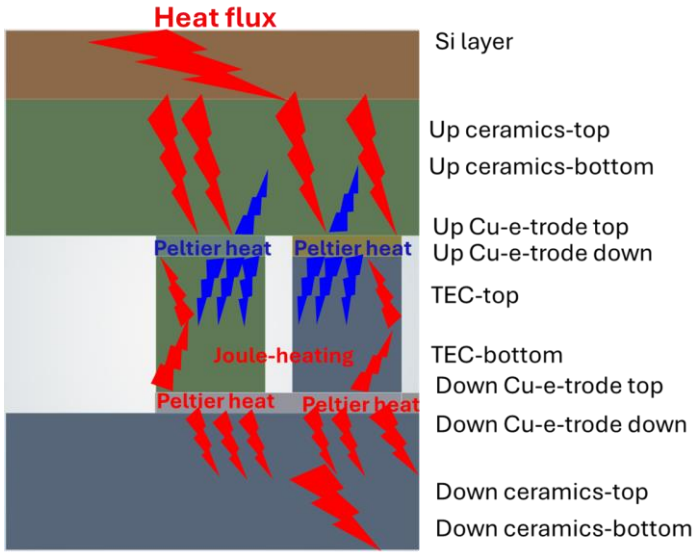


Between 0.1 and 1 second, the TEC effectively reduces the die temperature—demonstrating its active response time across a 100 µm Si wafer thickness

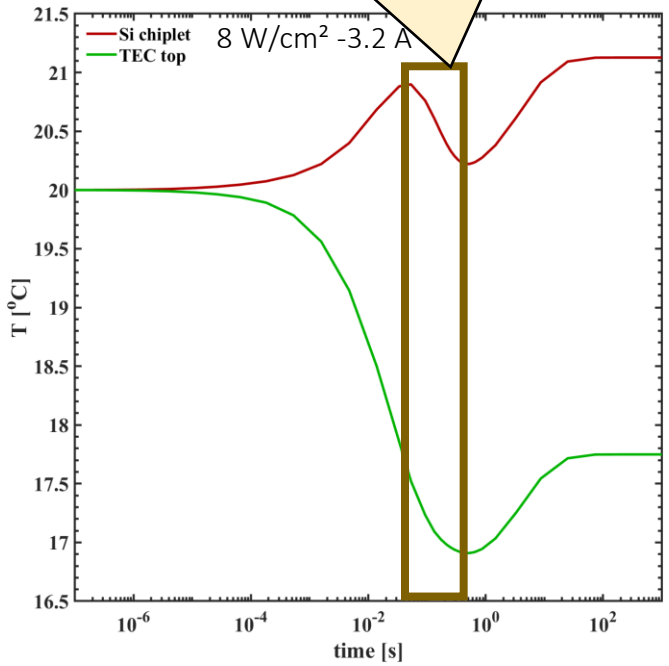


By operating the TEC under different conditions, we can actively modify the temperature profile and achieve greater uniformity across the wafer

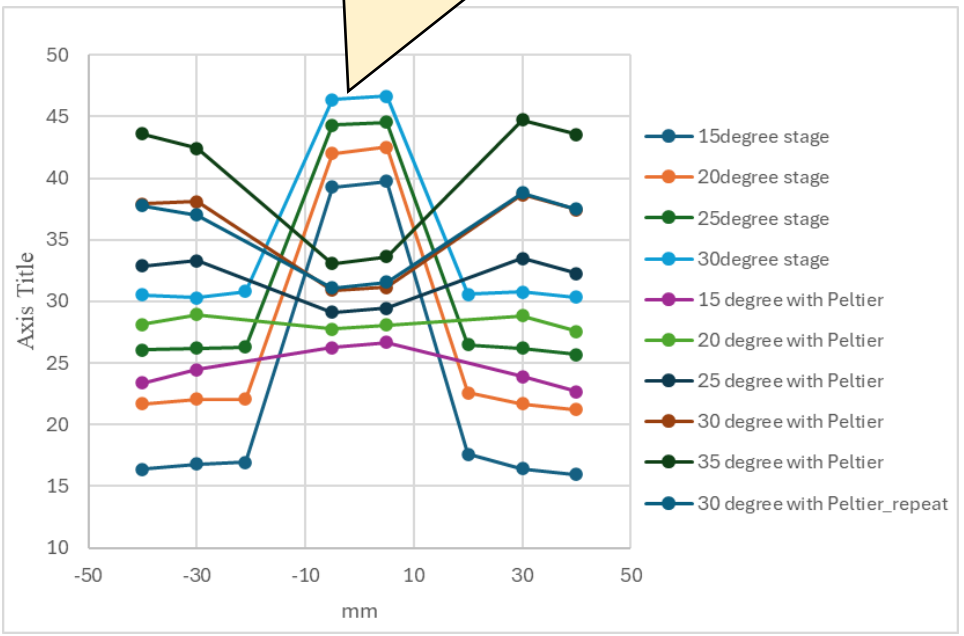


- With maximum heat power of 32 W , steady state within ΔT =1 °C achieved
- TECs are effective for fast, localized cooling, especially in short-duration thermal spikes during wafer-level testing

# Enhanced Cooling via Thin-Film Thermoelectric Elements

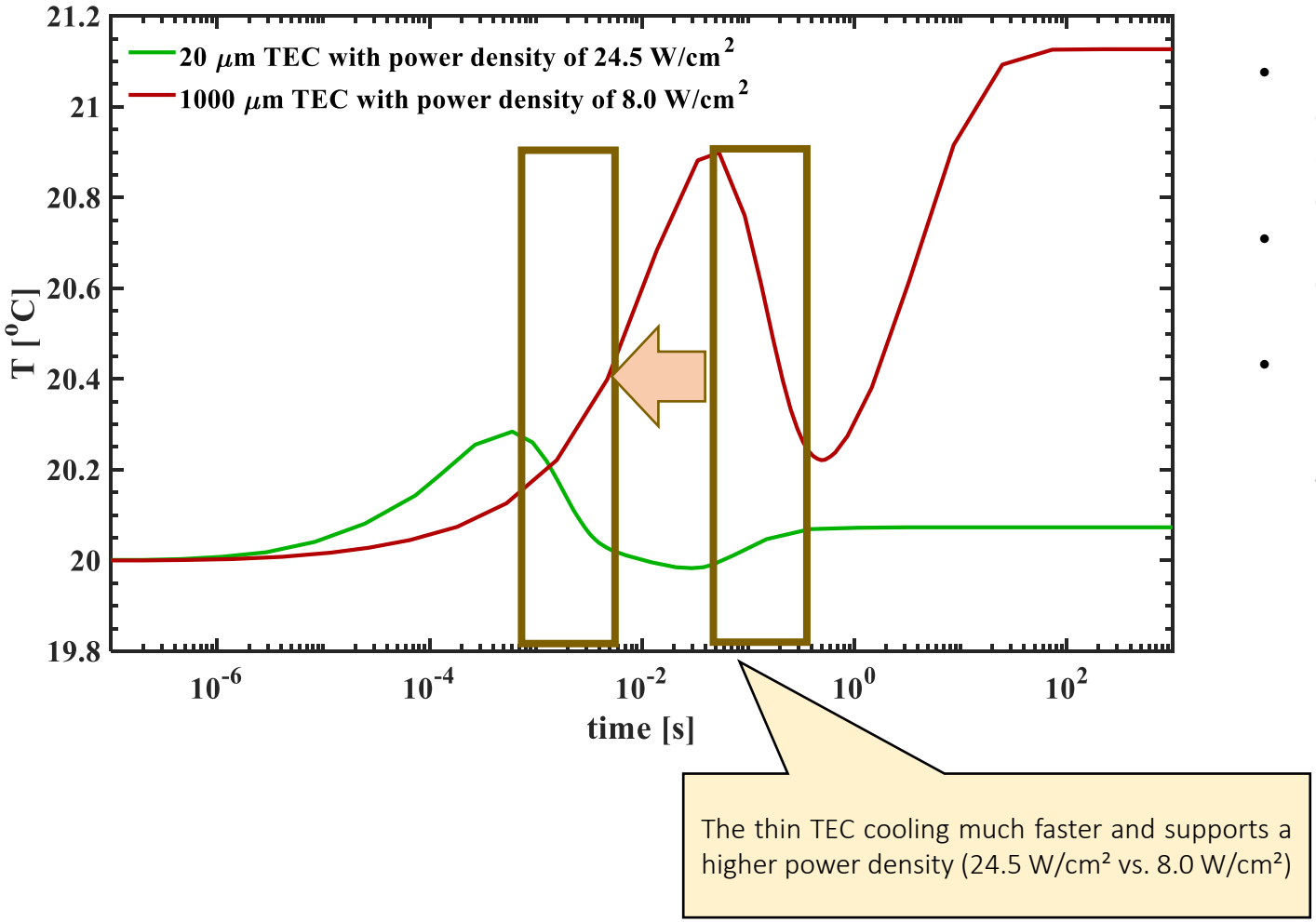


- Fast response - Commercially available TEC can have fast response to the temperature ~ depending to the applied heat flux and current
- Low heat flux - Commercially available TEC cannot remove the heat flux 1.25W/mm²~ maximum heat flux for TEC~100 times smaller
- Reducing the thickness of TEC 1000 µm to 20 µm each layer) can significantly increase the response time (~10 ms) and heat flux (24.5 W/cm²)

# Micro-Jet Impingement Array Approach

# Micro-Jet Impingement Cell Optimization

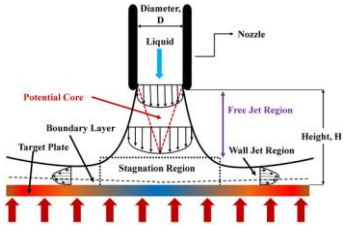


Micro-jet delivers high heat transfer coefficients and fast thermal response by directing small, high-speed fluid jets at localized hotspots

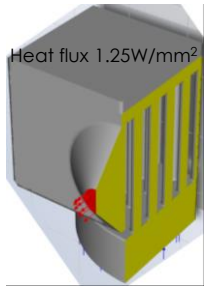


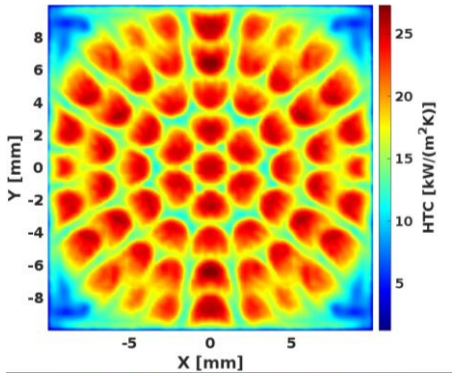


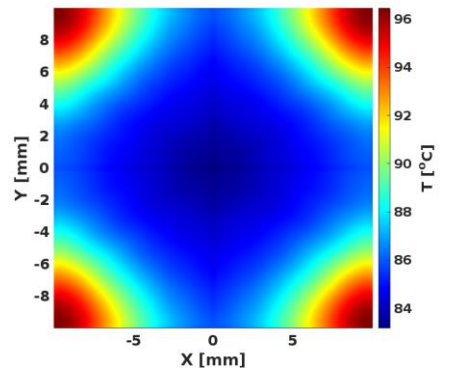


Large ΔT across the copper heat spreader ~ Not all area was covered with micro-jet

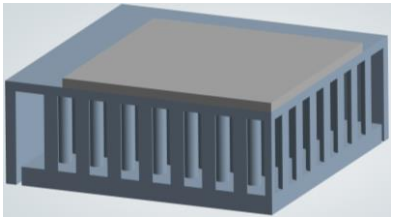

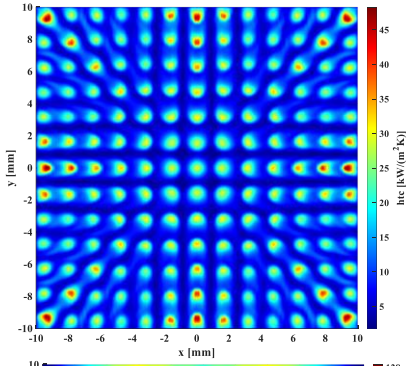


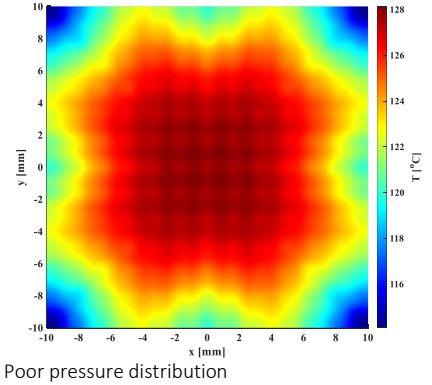


Poor pressure distribution
Non-uniform HTC across the jetting area
Lower HTC compared with circular shape
Large ΔT across copper heat spreader

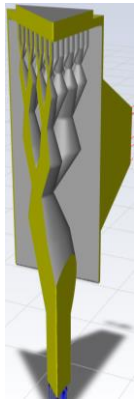

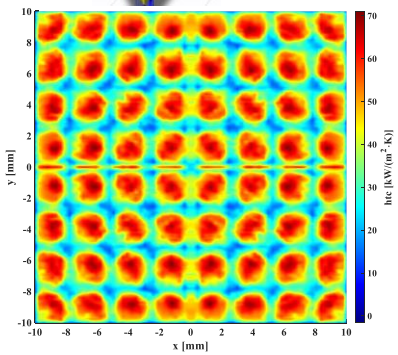


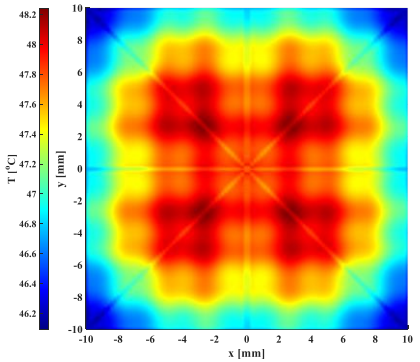


Optimized design of fractal channels ~ unform velocity distribution with low pressure drop
ΔT within 2 ° C better uniformity

# Performance Comparison: Thermoelectric vs. Micro-Jet Cooling

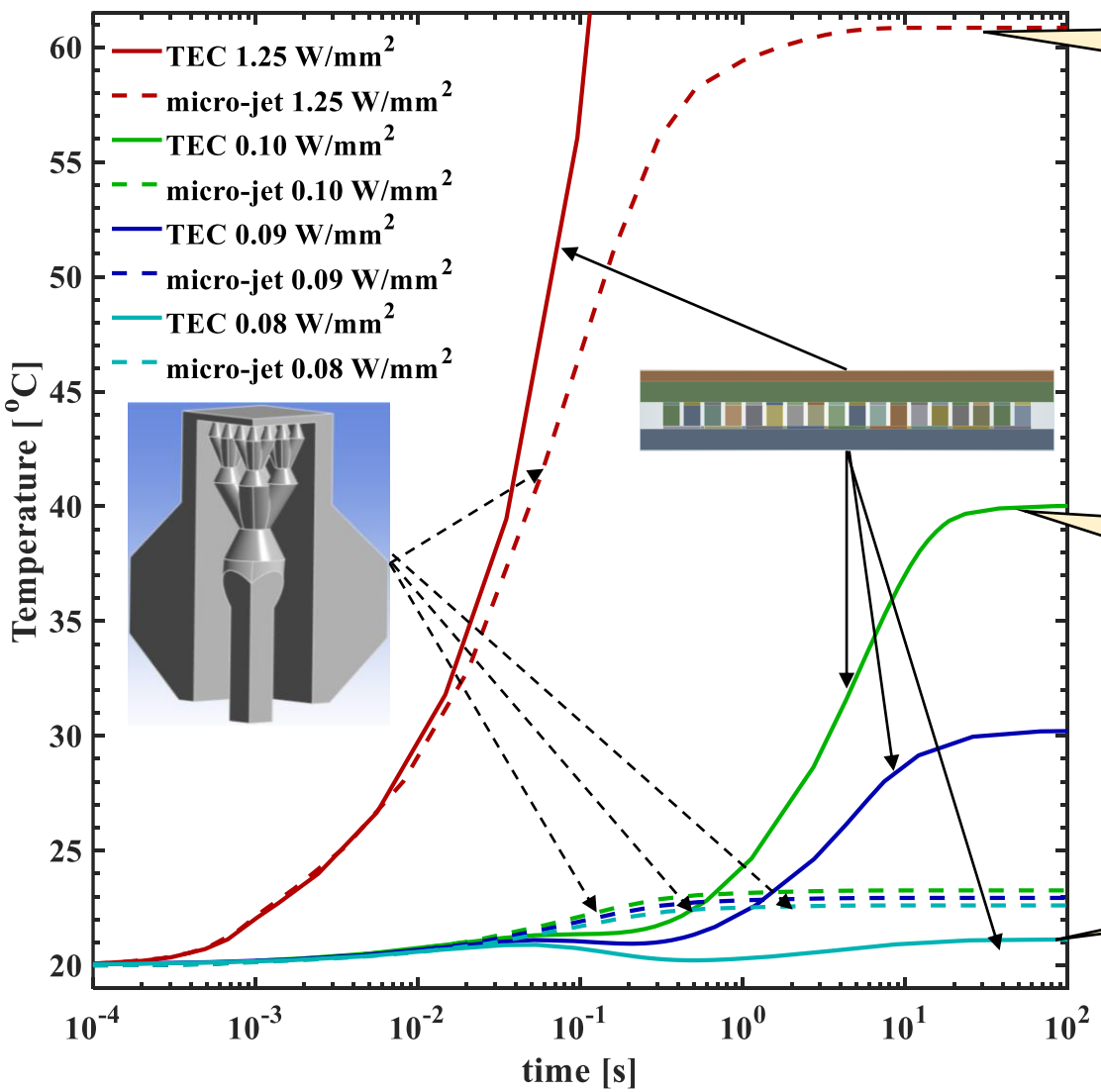


**Power Density ≈ 1.25 W/mm²:**
→ Micro-jet outperforms TEC in both response time and steady-state cooling

**Power Density ≈ 0.09-0.1 W/mm²:**
→ TEC still reacts faster initially,
→ but micro-jet achieves a lower steady-state temperature over time

**Power Density < 0.08 W/mm²:**
→ TEC responds faster and maintains a lower steady-state temperature than micro-jet cooling

TECs are effective for fast, low-power scenarios, micro-jets are more suitable for high-power, high-density applications

# Interposer Level Thermal Management

# Impact of Heat on Interposer

**Efficiency Losses:** Increased temperatures can degrade the efficiency of components and circuits, resulting in reduced power output, signal quality, and overall system performance.

**Signal Distortion:** Heat-induced thermal variations can cause changes in the electrical properties of RF components, leading to signal distortion, phase shifts, and frequency drift.

**Reliability Issues:** Excessive heat can accelerate the degradation of electronic components and materials, leading to premature wear-out, thermal fatigue, and reliability issues. Thermal stress and thermal cycling can cause solder joint failures, interconnect delamination, and semiconductor breakdown, compromising system reliability and longevity.

**Thermal Runaway:** In extreme cases, excessive heat accumulation can trigger thermal runaway phenomena, where temperature increases uncontrollably, leading to catastrophic failure or damage to components and systems.

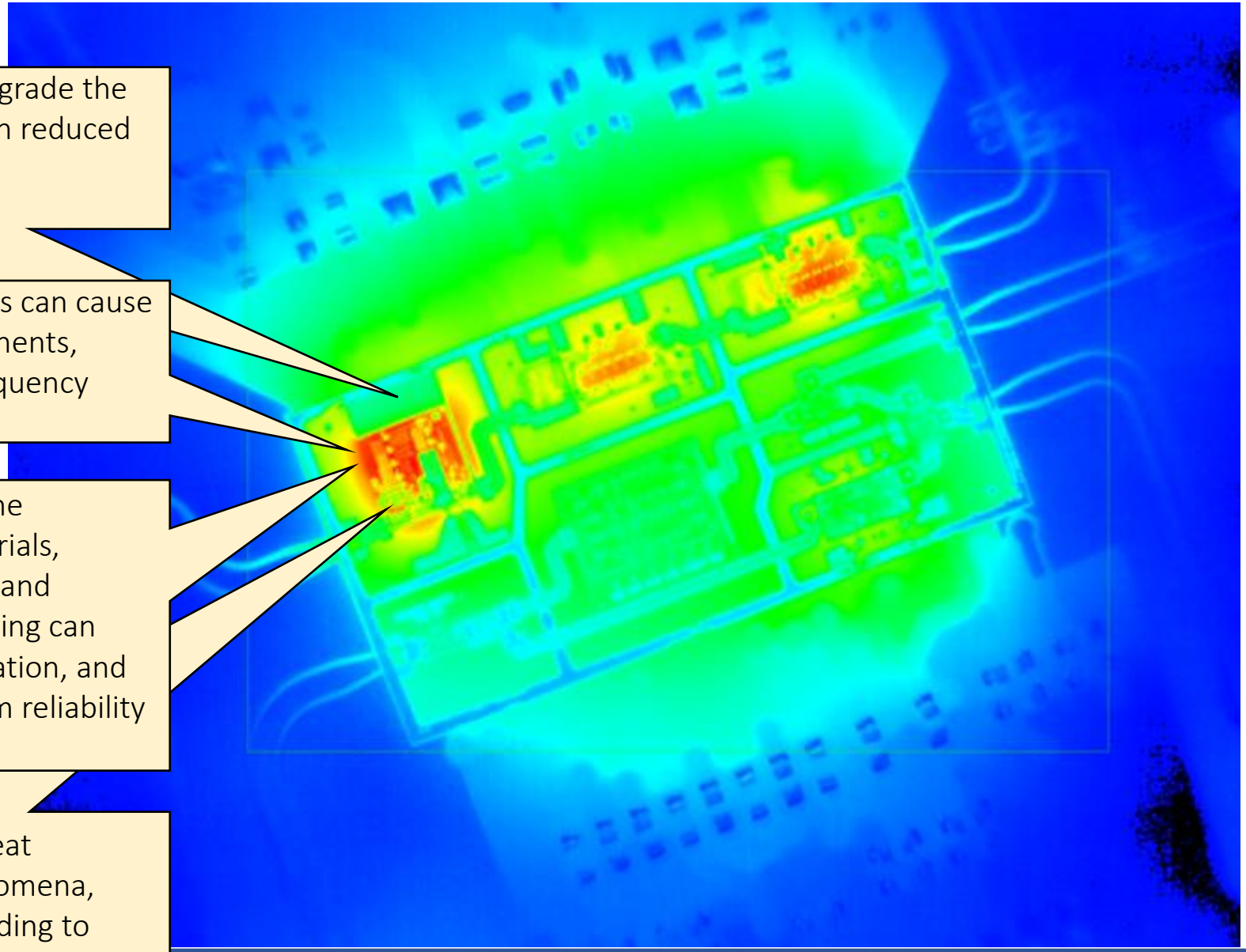

# Material Requirements for High-Performance Interposers

- **High Thermal Conductivity**

Substrate materials with high thermal conductivity facilitate the efficient transfer of heat away from the active components, thereby maintaining optimal operating temperatures.

- **Low Dielectric Loss**

Materials with low dielectric loss properties help preserve signal integrity and reduce RF losses, enabling efficient transmission of high-frequency signals.

- **High Electrical Insulation**

Effective electrical insulation properties are necessary to prevent short circuits and interference between different components or conductive traces on the substrate. Insulating materials help maintain signal isolation and prevent unintended electrical coupling, ensuring reliable operation of RF circuits.

- **Wide Bandgap**

Wide bandgap materials exhibit excellent breakdown voltage characteristics, making them suitable for high-power operation without compromising reliability.

- **Mechanical Stability**

Substrate materials should possess mechanical stability to withstand the stresses and strains encountered during fabrication, assembly, and operation.

- **Cost-Effectiveness**

Balancing performance with cost considerations is essential to meet the economic requirements of high-volume production in RF applications.

# Interposer Substrate Material Properties

| Material | Bandgap (eV) | Critical Electric Field (MV/cm) | Thermal Conductivity (W/mK) | On-Resistance (mOhm·cm²) | Breakdown Voltage (kV/mm) | Melting point (°C) |
|---|---|---|---|---|---|---|
| **Si** | 1.1 [1] | 0.3 - 1.0 [2] | 150 - 200 [3] | 1 - 100 [4] | 0.2 - 0.7 [5] | 1,414 [30] |
| **SiC** | 3.2 [6] | 2.2 - 4.5 [7] | 250 - 300 [8] | 0.1 - 10 [9] | 2.5 - 4.7 [10] | 2,830 [31] |
| **GaN** | 3.4 [11] | 2.5 - 3.3 [12] | 130 - 180 [13] | 0.1 - 10 [14] | 2.6 - 3.3 [15] | 1,100 [32] |
| **GaAs** | 1.4 [16] | 3 - 6 [17] | 50 - 60 [18] | 0.1 - 10 [19] | 0.2 - 0.8 [20] | 1,237 [33] |
| **Diamond** | 5.5 [25] | 20 [26] | 2000 - 2200 [27] | 0.01 - 1 [28] | >5 [29] | 3,550 [35] |

- Very expensive
- Difficult material to grow and process
- High density of defects
- Very hard material -> difficult to form reliable electrical contacts
- High electrical resistance -> difficult to form low-resistance contacts


[1] L. T. Canham, "Silicon quantum wire array fabrication by electrochemical and chemical dissolution of wafers," Appl. Phys. Lett. 57, 1046 (1990).
[2] H. P. Maruska and J. P. W. Yoon, "Epitaxial growth of silicon carbide," J. Appl. Phys. 32, 250 (1961).
[3] R. A. Powell and H. J. Schulz, "Thermal conductivity of silicon and germanium from 3°K to the melting point," Phys. Rev. 83, 1271 (1951).
[4] K. T. Short, C. J. R. Sheppard, and M. E. Law, "On the specific contact resistance of metal contacts to silicon," Appl. Phys. Lett. 58, 2791 (1991).
[5] M. J. Kumar and J. J. Liou, "Analysis of MOS-gated power rectifiers," IEEE Trans. Electron Devices 39, 1414 (1992).
[6] M. K. Das, "Crystallographic etching of SiC," J. Electrochem. Soc. 127, 2363 (1980).
[7] S. K. Ryu, K. Y. Lee, S. K. Kim, and G. T. Kim, "High critical electric field strength of 4H-SiC MOS capacitors," Solid State Electron. 47, 1679 (2003).
[8] R. P. Devaty and W. J. Choyke, "Hexagonal silicon carbide - a review," J. Mater. Sci. 36, 2835 (2001).
[9] S. Yoshida, H. Sato, and H. Matsunami, "Silicon carbide (SiC) MOSFET technology and its applications," IEEE Trans. Power Electron. 36, 2438 (2021).
[10] J. Zhang, M. J. O'Loughlin, C. D. Brandt, and M. Skowronski, "Vertical MOSFETs in 4H-SiC with high voltage and low on-resistance," IEEE Electron Device Lett. 23, 131 (2002).
[11] R. Collazo and Z. Sitar, "GaN-based power electronic devices," MRS Bull. 39, 523 (2014).
[12] T. Egawa, T. Jimbo, H. Ishida, and M. Umeno, "GaN power devices: Current status and future prospects," Proc. IEEE 101, 2122 (2013).
[13] J. H. Kim and B. J. Baliga, "Comparison of silicon and GaN power devices for future power electronics applications," IEEE Trans. Electron Devices 60, 1739 (2013).
[14] M. A. Khan, A. M. A. Hafiz, and S. M. Islam, "Gallium nitride (GaN) power devices: A review," Energies 11, 1662 (2018).
[15] S. S. Wong, S. H. Chen, P. T. Lai, K. Y. Choy, and K. W. Cheng, "Low-resistance lateral GaN Schottky diode with improved breakdown voltage and reverse leakage by selective etching," IEEE Electron Device Lett. 30, 1057 (2009).
[16] R. C. Newman, "Bandgap engineering and device applications of GaAs and related alloys," Journal of Electronic Materials, vol. 24, no. 4, pp. 359-370, 1995.
[17] S. Nakamura, "GaN-based ultraviolet LEDs and their applications to solid-state lighting and full-color displays," Journal of Physics D: Applied Physics, vol. 48, no. 1, p. 013001, 2014.
[18] E. P. O'Reilly, "III-V nitride semiconductors and their alloys," Reports on Progress in Physics, vol. 66, no. 2, pp. 239-303, 2003.
[19] S. L. Chuang, Physics of Optoelectronic Devices, John Wiley & Sons, Inc., 1995.
[20] J. Singh, "Gallium arsenide and related compounds," in Electronic and Optoelectronic Properties of Semiconductor Structures, Cambridge University Press, 2003, pp. 19-67.
[25] J. E. Butler and L. C. Feldman, "The electronic properties of diamond," Advances in Physics, vol. 22, no. 4, pp. 517-550, 1973.
[26] S. S. Batsanov, "Electronic properties of diamond," Physics-Uspekhi, vol. 40, no. 10, pp. 1035-1058, 1997.
[27] D. J. Twitchen and M. L. Markham, "The properties and applications of diamond," Annual Review of Materials Science, vol. 29, pp. 327-368, 1999.
[28] P. E. Petit, R. P. Devaty, and W. J. Choyke, "Electrical properties of diamond," Materials Science and Engineering: R: Reports, vol. 21, no. 6, pp. 171-223, 1998.
[29] S. Nakamura and G. Fasol, The Blue Laser Diode: The Complete Story, Springer Science & Business Media, 2000.
[30] R. W. Schwartz, "Melting Point of Silicon from 1000 to 1500 °C," Journal of Research of the National Bureau of Standards, vol. 53, no. 6, pp. 365-369, Dec. 1954.
[31] H. L. Tuller and R. C. Bradt, "The Effect of Impurities on the High-Temperature Mechanical Properties of Silicon Carbide," Journal of the American Ceramic Society, vol. 56, no. 10, pp. 537-539, Oct. 1973.
[32] D. K. Schroder, Semiconductor Material and Device Characterization, 3rd ed. Hoboken, NJ: John Wiley & Sons, 2006.
[33] G. A. Slack, "New Thermal Conductivity Measurements for Solids at High Temperatures," Journal of Physical and Chemical Reference Data, vol. 34, no. 1, pp. 1-34, Jan. 2005.
[35] J. E. Field, The Properties of Natural and Synthetic Diamond. London, U.K.: Academic Press, 1992.

# Si/SiC Hybrid Bonding Techniques

## Plasma assisted bonding

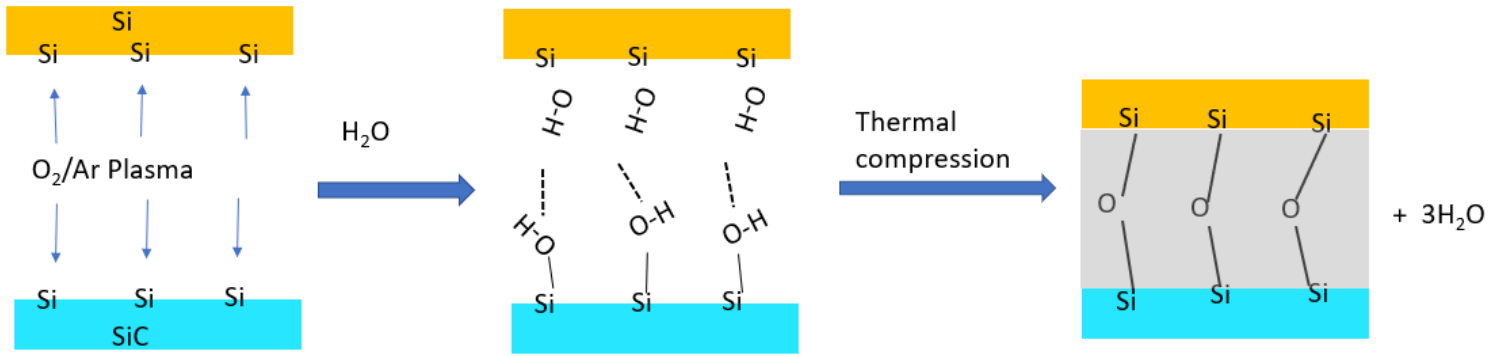


**Plasma activation**

$Si^{\bullet} + HO\text{-}H + SiO^{\bullet} \rightarrow Si\text{–}OH + HO\text{–}Si$

**Thermalcompression**

$Si\text{–}OH + HO\text{–}Si \rightarrow Si\text{–}O\text{–}Si + HOH$

**Water treatment**

$Si\text{–}O\text{–}Si + HOH \rightarrow Si\text{–}OH + HO\text{–}Si$

## Bonding with Al interface

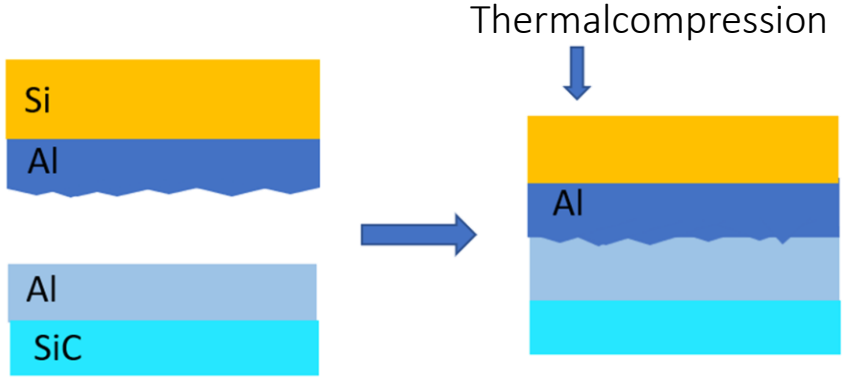


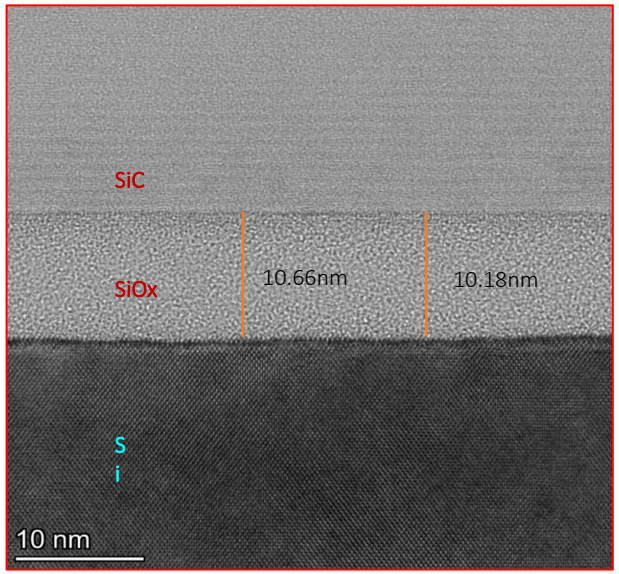


**Direct bonding advantage:**
Avoid metal incorporation, electrical leakage, and RF signal loss

**Challenges:**
1) Bonding should be done at low temperature (< 400C), surface roughness should be very small (Rq<10nm)
2) Low press force to avoid the damage to the patterned area

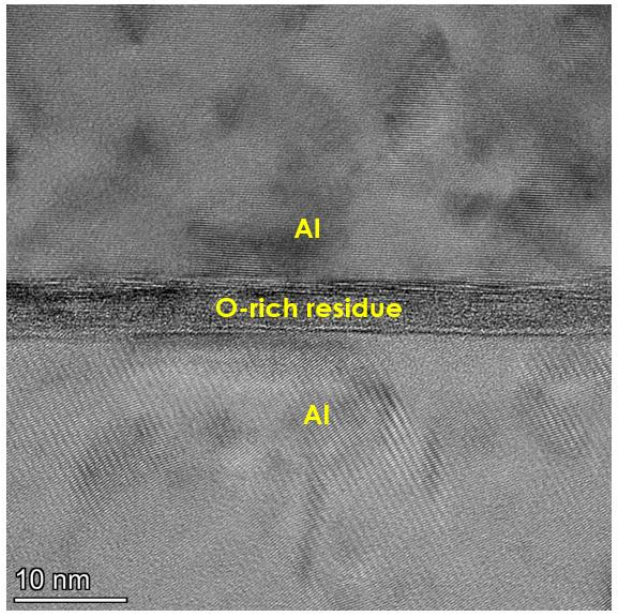


**Bonding with Al interface advantages:**
1) Bonding at low temperature (< 250degree)
2) Surface roughness is not critical
3) Low press force

# Thermal Performance Comparison of Hybrid Bonded Si/SiC

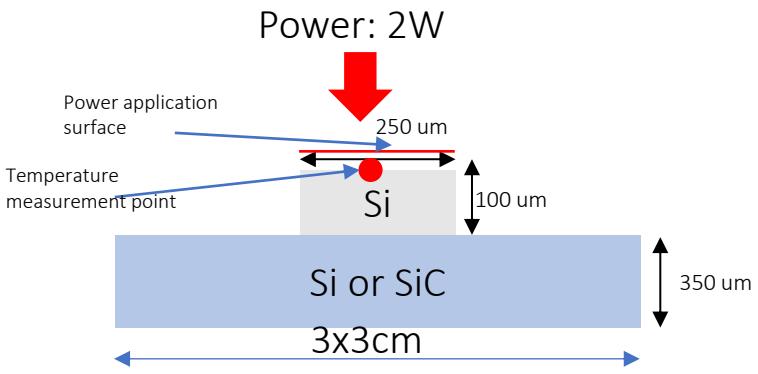


1. Si or SiC

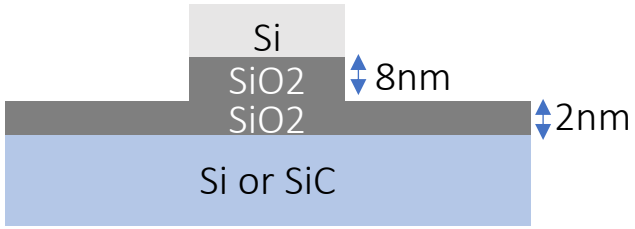


2. Si or SiC, $SiO_2$ layer

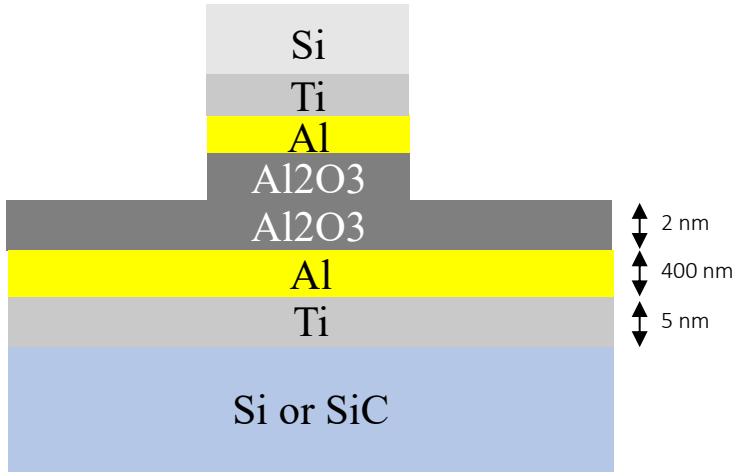


3.Si or SiC, Al, $Al_2O_3$ layers

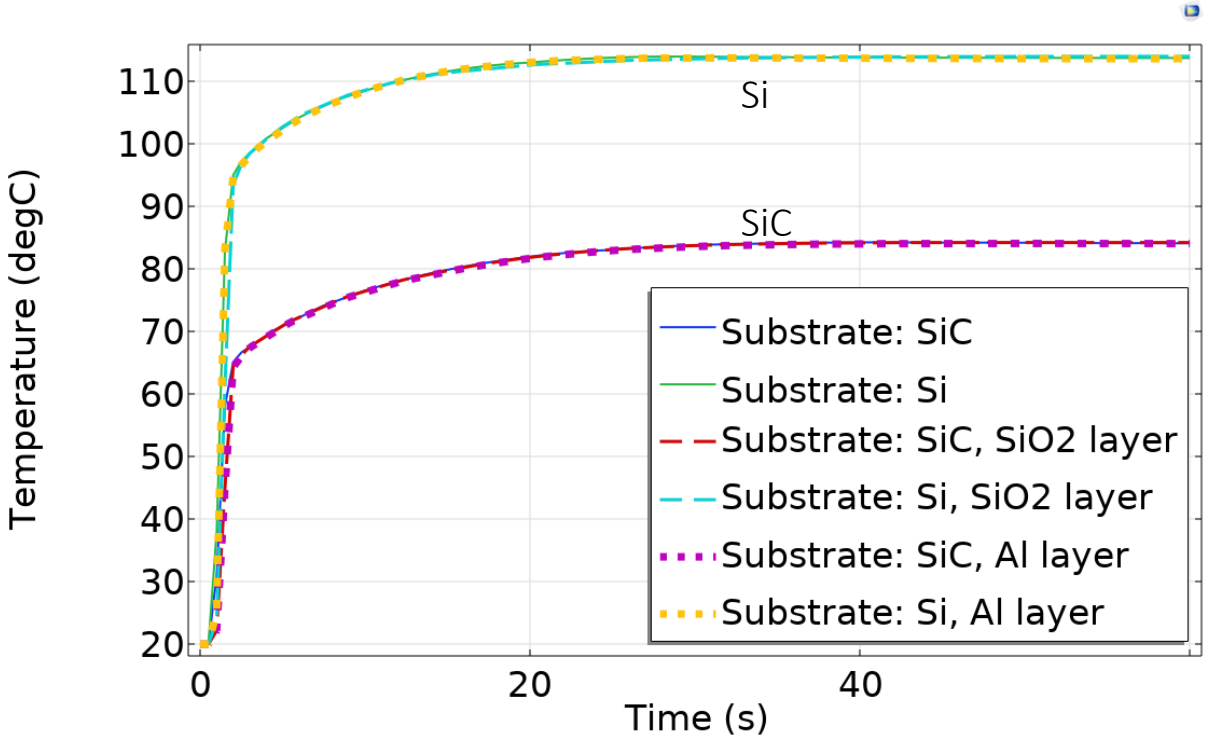


Simulation was done using COMSOL

Assumption:
1. Free-standing
2. Natural convection on all the surfaces
3. Neglect radiation

SiC substrates lower hotspot temperatures by up to 26% versus Si, giving us the flexibility to choose bonding methods based on other factors like cost or integration ease

# SiC Interposer Enables Higher Component Density

Keep max temperature on Si die as 70°C

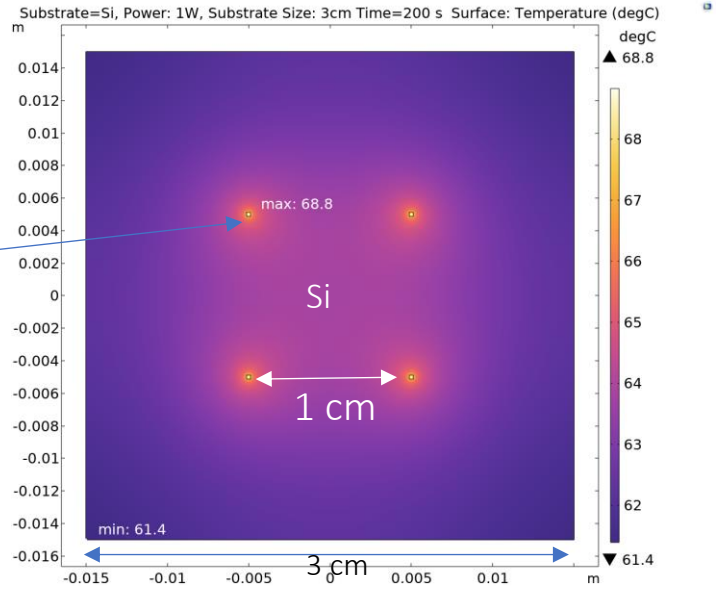


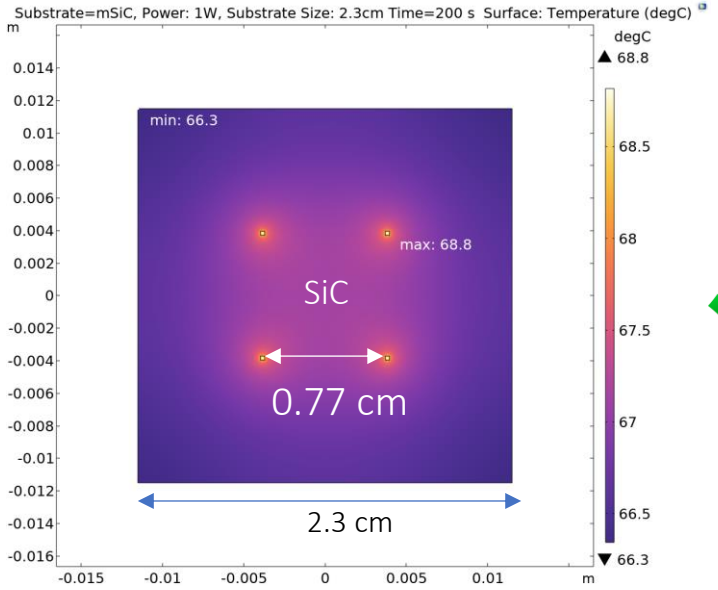


✓ Component density increased by 23.3%

Keep max temperature on Si die as 170°C

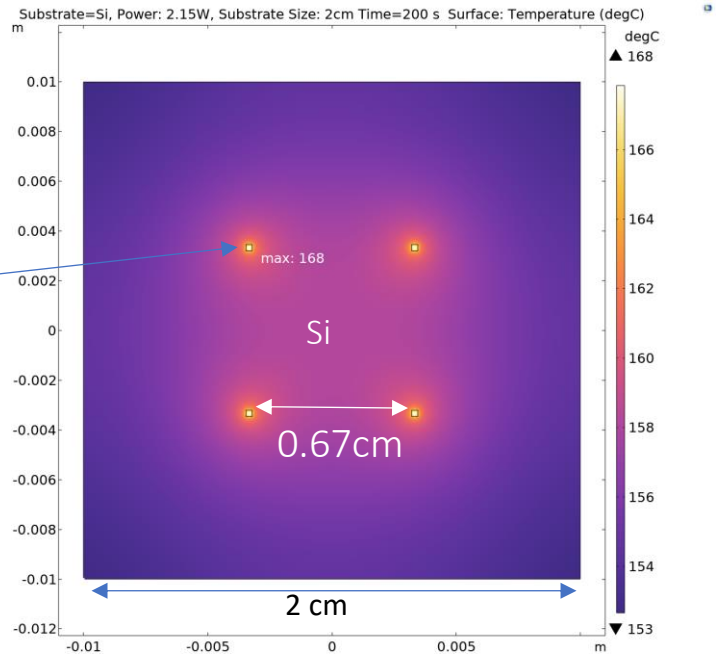


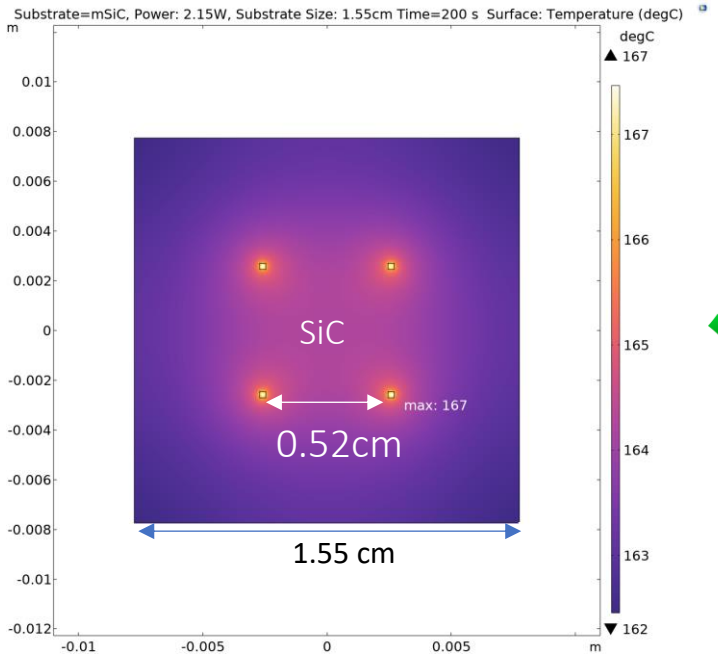


✓ Component density increased by 22.5 %

# Integrated Cooling Methods for Higher Density Interposers

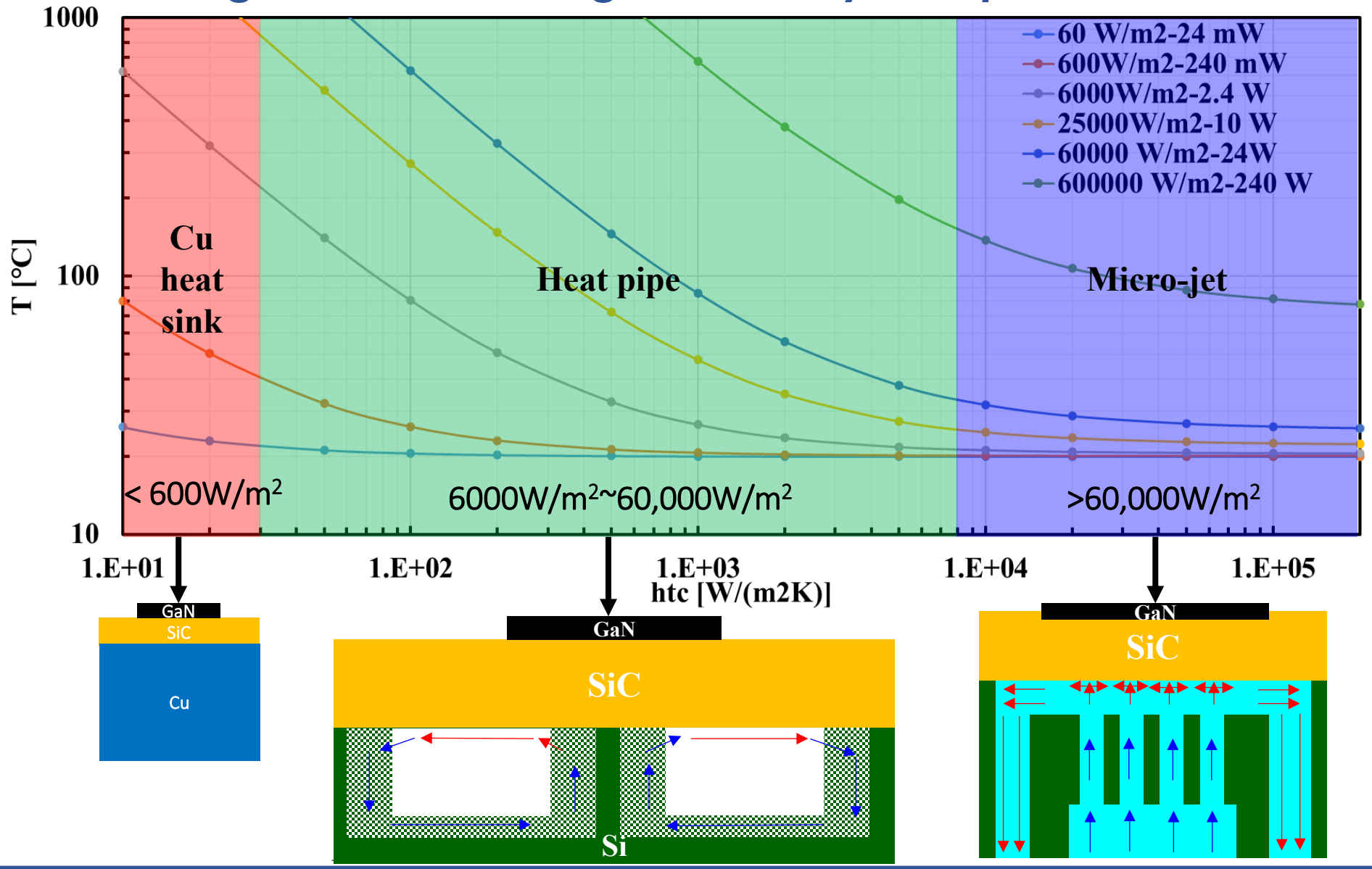


By tailoring the cooling method to the application's power density, we can enable high-performance, thermally stable interposer platforms for advanced IC packaging

# PCB Level Thermal Management:

# Passive Thermal Management Solution

# Thermal Challenges in Flexible PCB

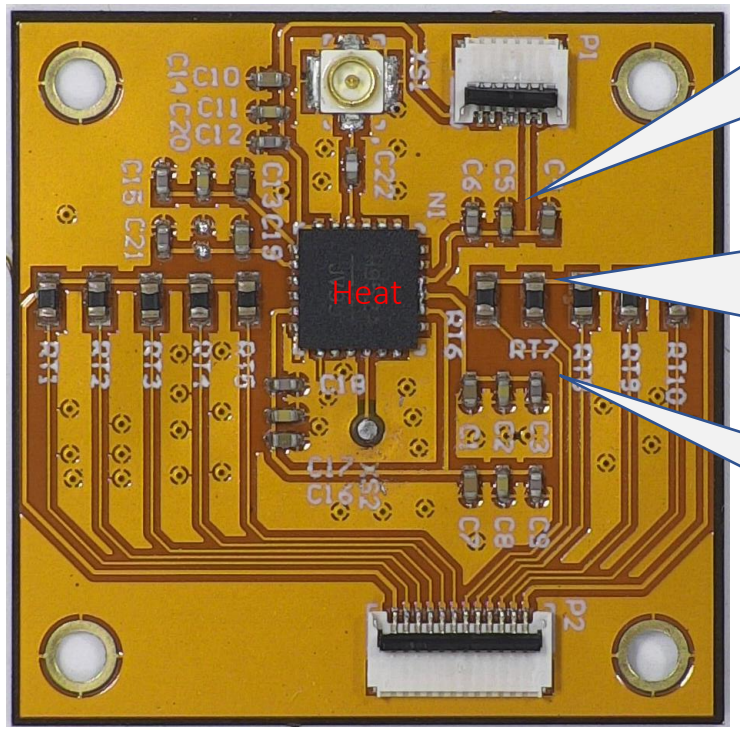


**Hotspot Formation:**

- Uneven heat distribution can lead to localized hotspots on PCB. These hotspots not only affect the performance of nearby components but can also cause damage to the PCB material.

**Mechanical Stress:**

- Elevated temperatures can lead to thermal expansion of the flexible PCB materials. This expansion and contraction cycle can induce mechanical stress and strain, potentially leading to material degradation and compromised mechanical integrity.

**Integration Complexity:**

- Integrating efficient thermal management solutions without compromising the flexibility of the PCB and the overall mechanical design can be challenging.
- The compact form factor of flexible PCBs limits the available space for heat management solutions. Designing efficient solutions that fit within these constraints is challenging.

# Temperature Impact on RF Components

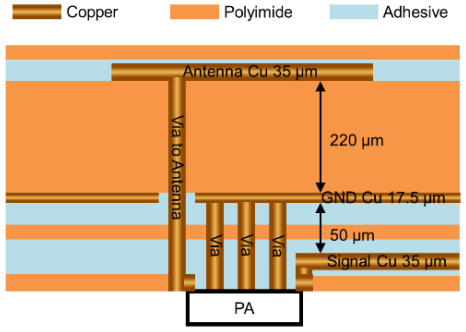


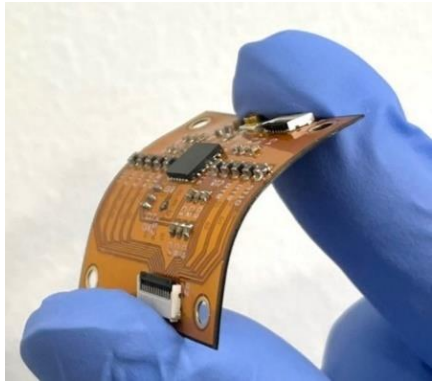

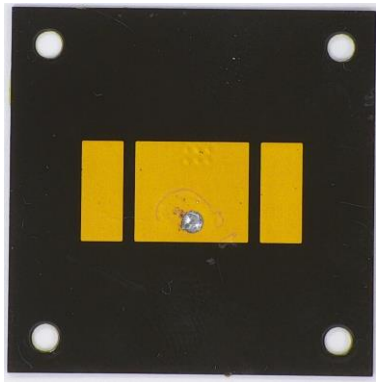

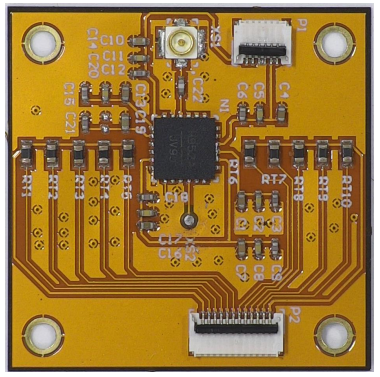

Antenna integration platform design

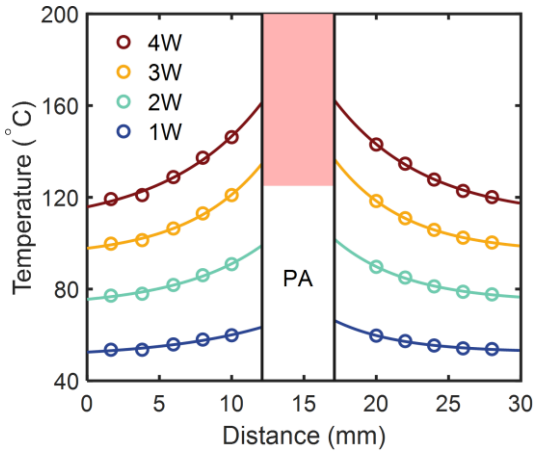


Temperature distribution on the PCB

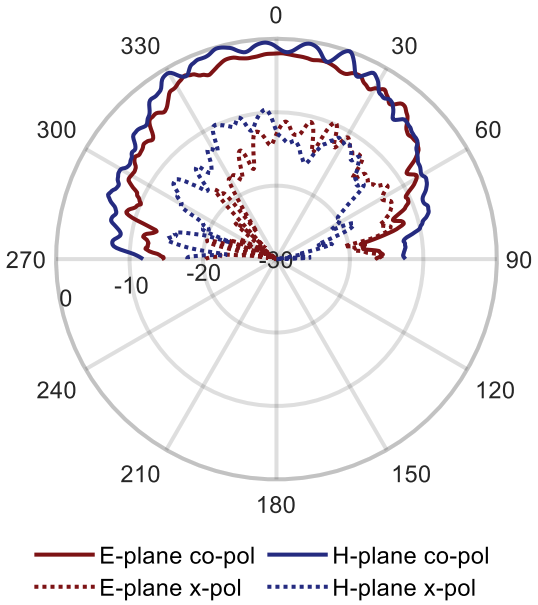


Radiation patterns at the resonance frequency

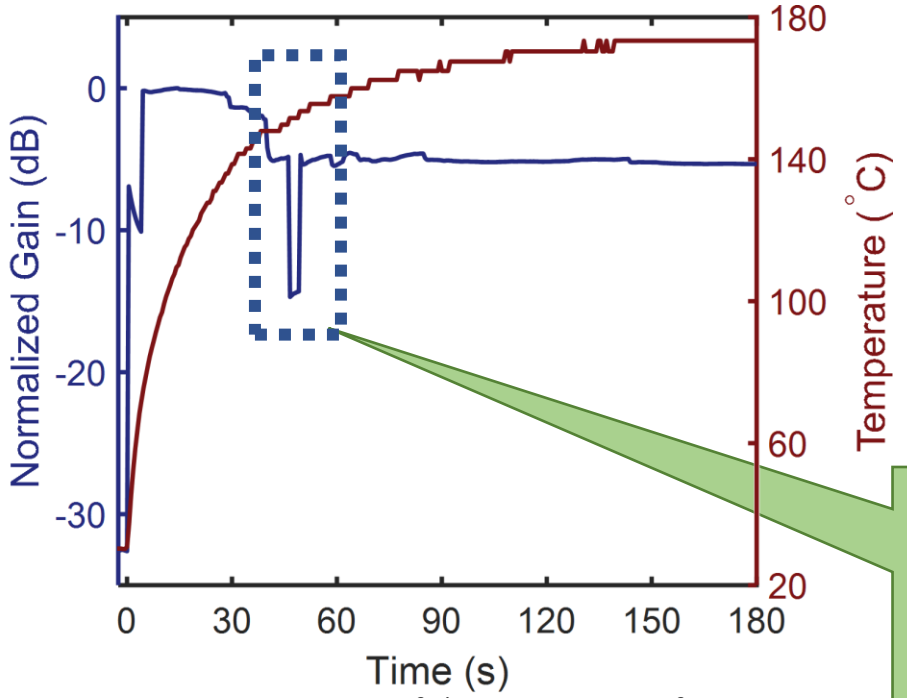


Temperature impact of the antenna performance

PA: HMC952ALP5GE (ADI)

- 26% PAE
- 32 dB gain
- 8-14 GHz

PA forced to operate in a safer but **less efficient** mode, after **self-protection** loop was triggered by temperatures, otherwise **burn**

# Design and Characterizations of PCB With the Thermal Management Structure

a

Without thermal management

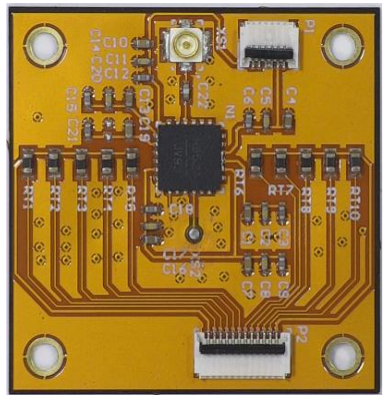

d

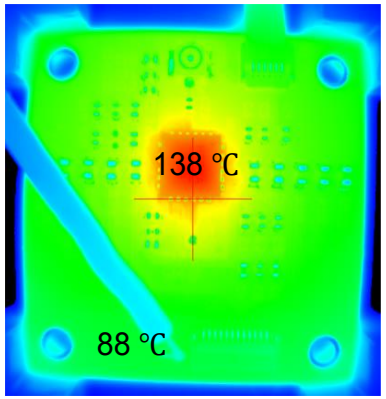


b

With insulation and heat spreading layer

e

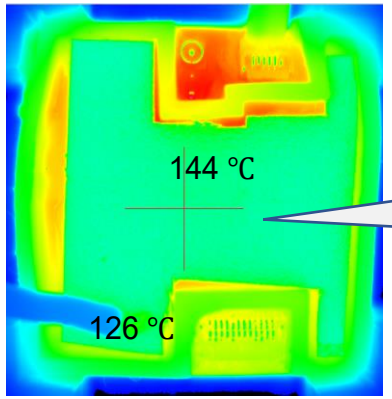


Surface temperature distribution became more uniform

c

Fully equipped with the proposed thermal management solution

f

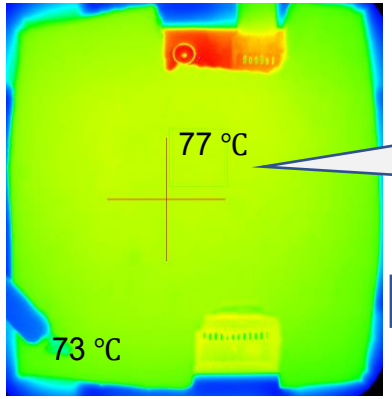


Overheating is delayed, and the equilibrium temperature is reduced

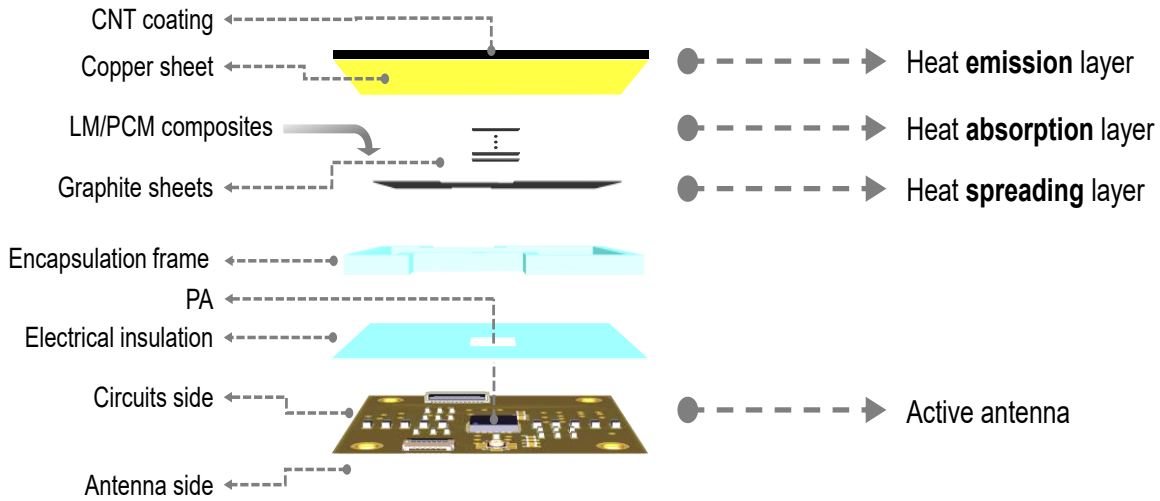


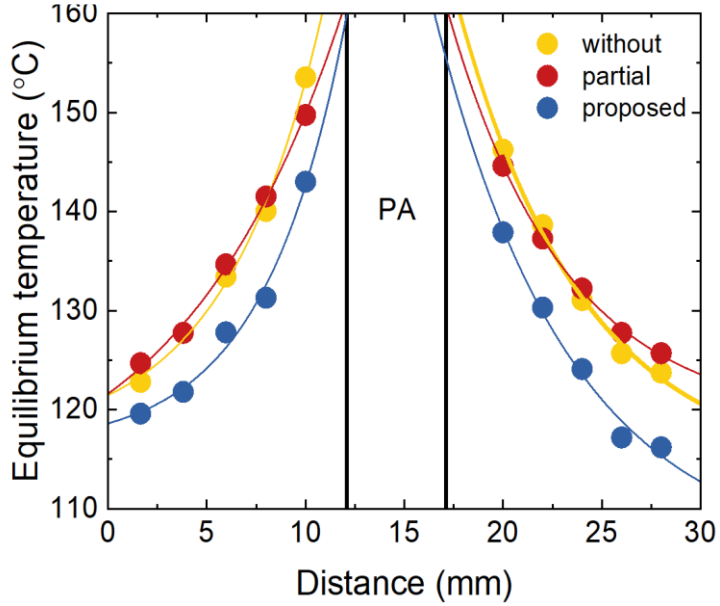


Equilibrium temperature distribution along the thermistor array

# Thermal Management Concept: Combination of Heat Spreading, Heat Adsorption, and Radiation Materials for Optimal Performance

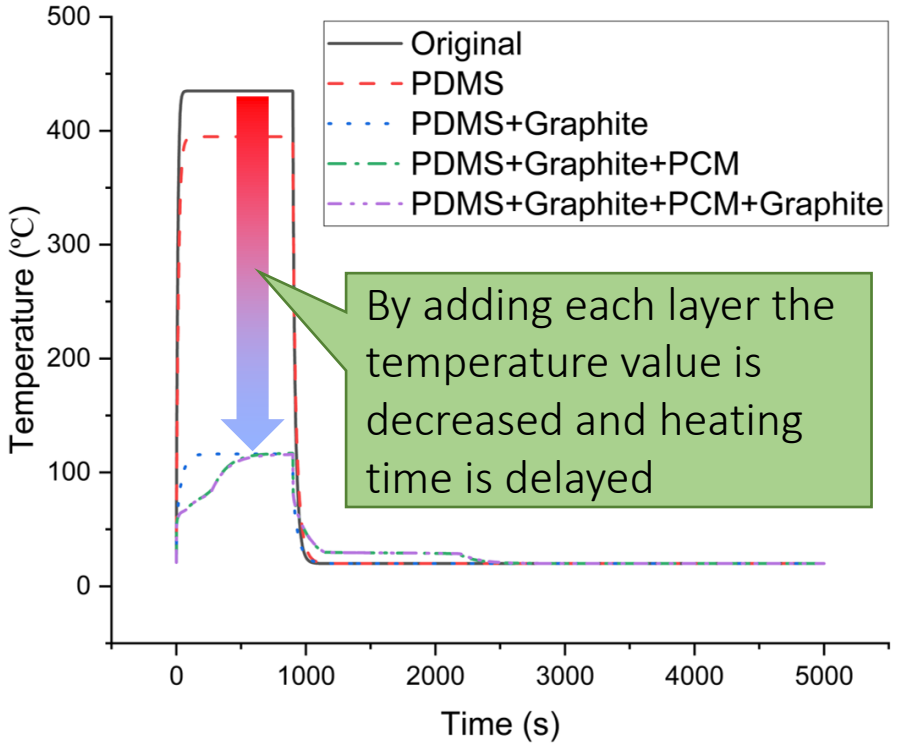


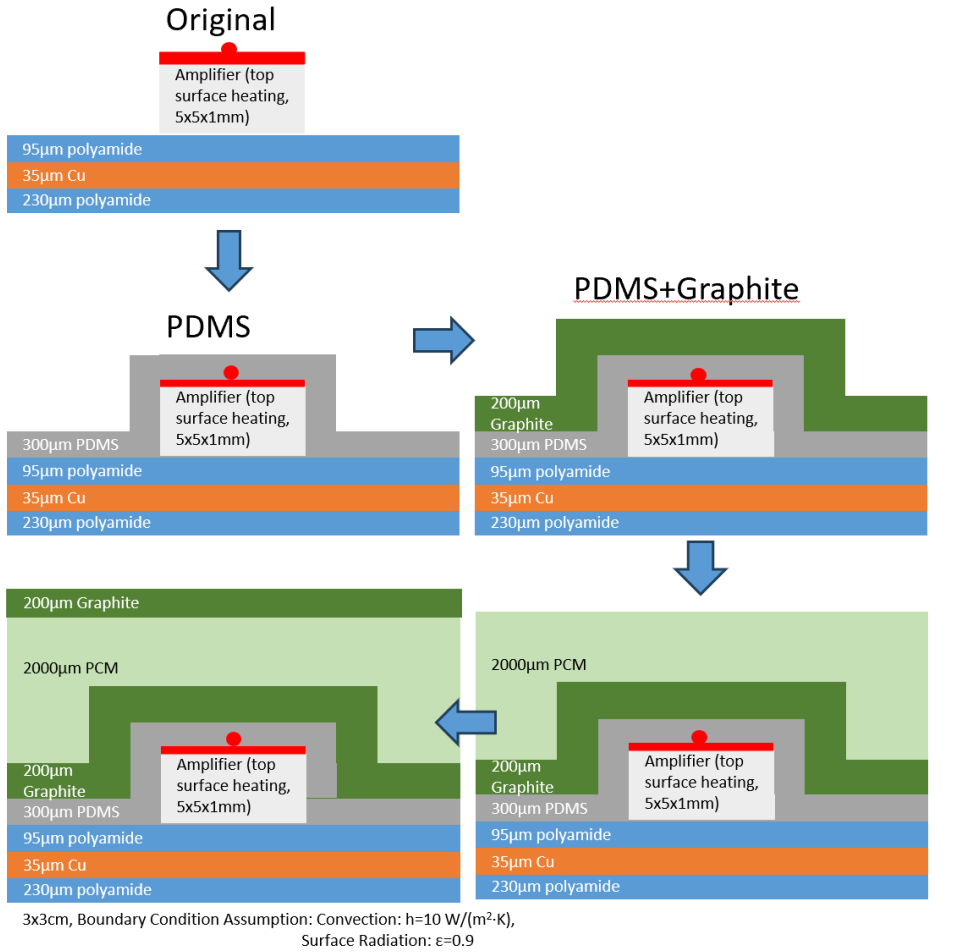

# Material Evaluation for Passive Heat Spreading

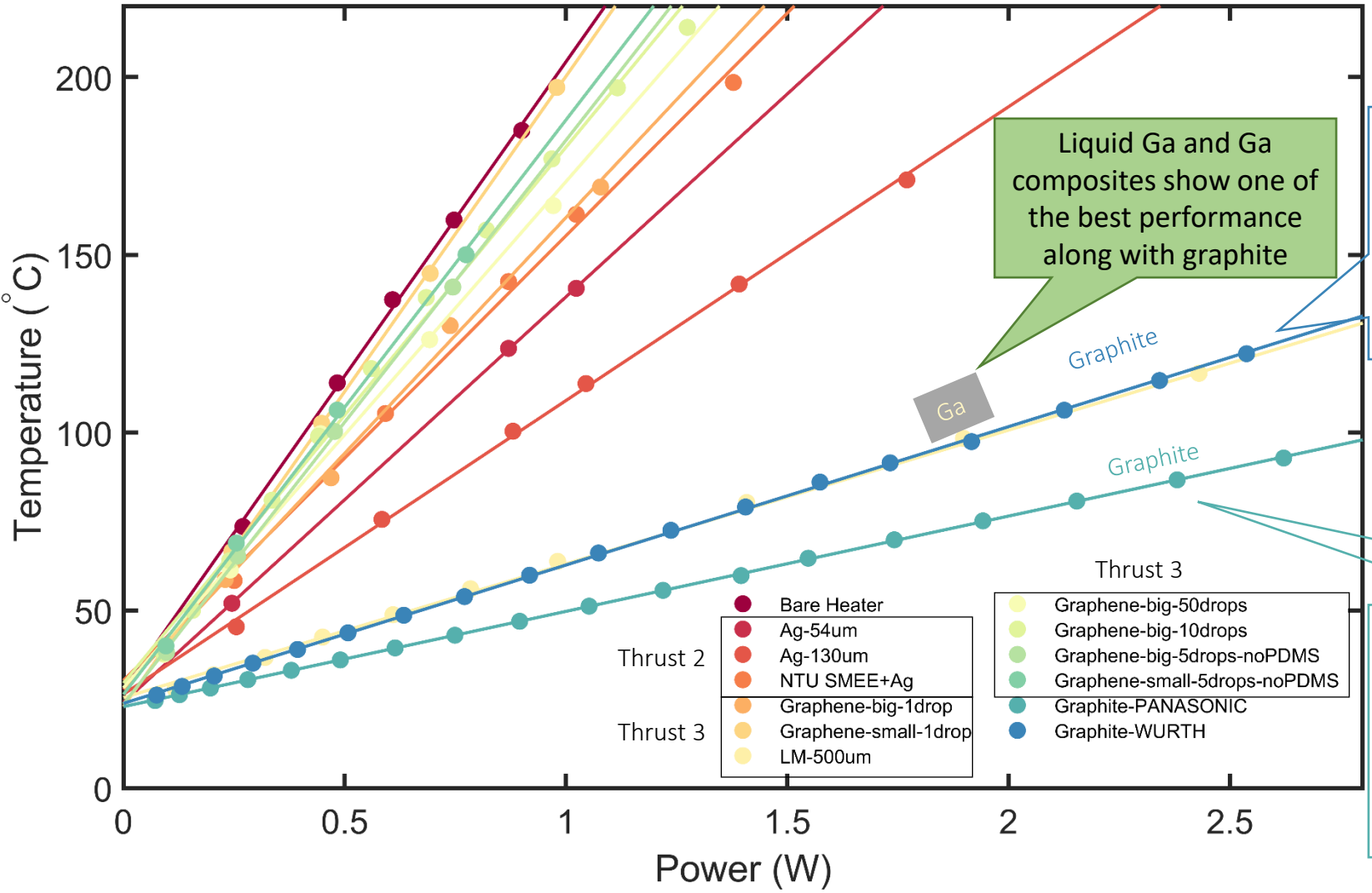


Temperature distribution at ~2.5W

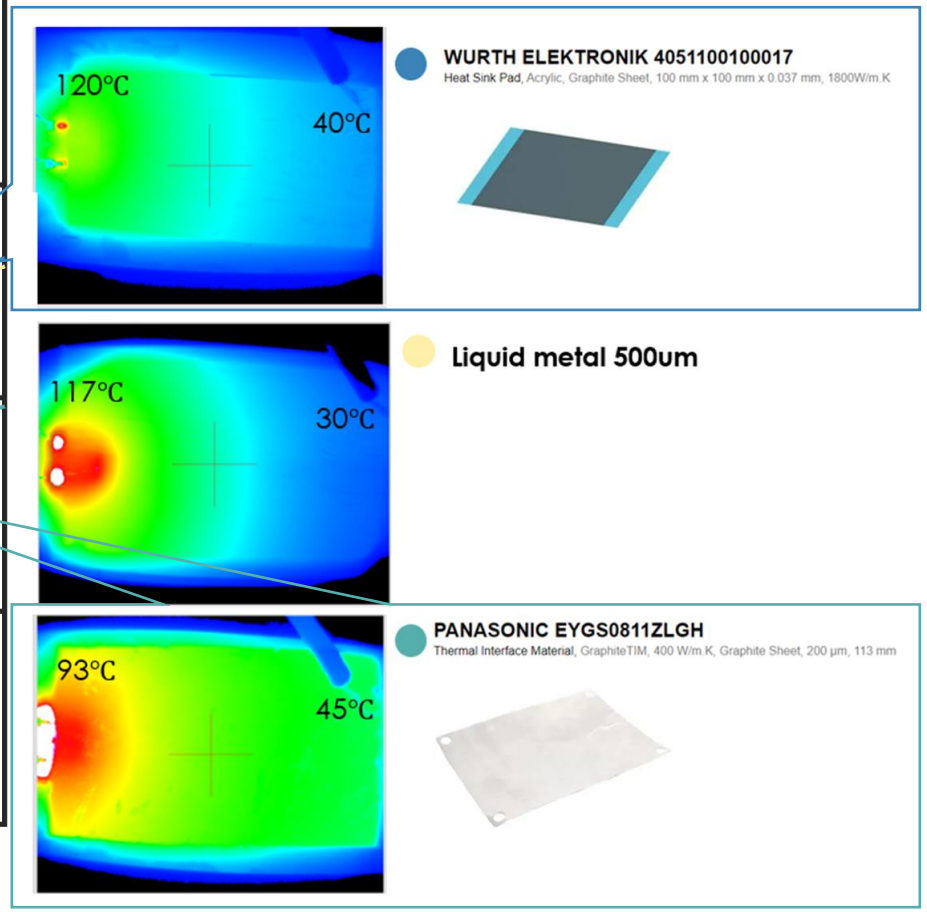




28

# Material Trade-offs: Ga:PCM Composite

## Liquid Ga

- Good thermal conductivity
  - 21 W/mK @ 20 ℃
  - 16 W/mK @ 40 ℃
- Low heat capacity

## PCM n-Octadecane

- Large heat capacity
  - 2.7 J/gK @ 40 ℃ (liquid)
- Absorb even **larger latent heat** during melting
  - 222 J/g
- low thermal conductivity
  - 0.11 W/mK @ 20 ℃ (solid)
  - 0.16 W/mK @ 40 ℃ (liquid)

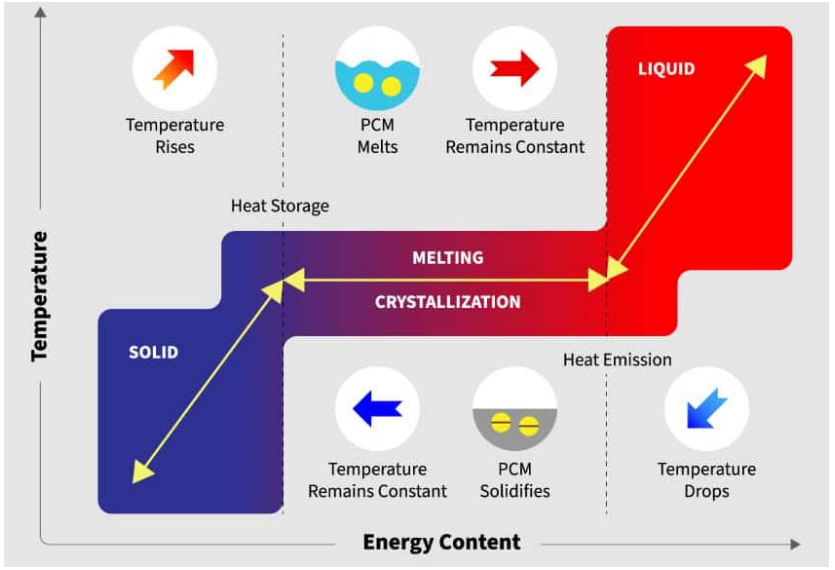


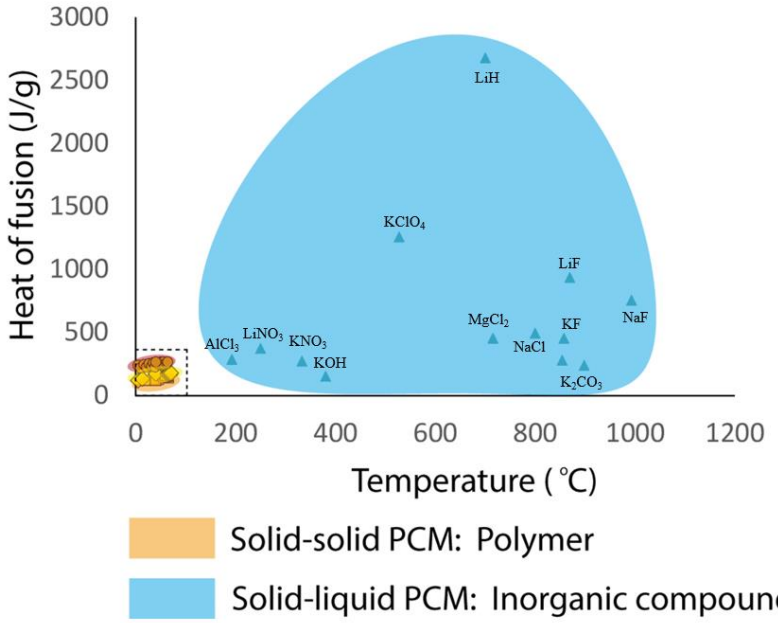


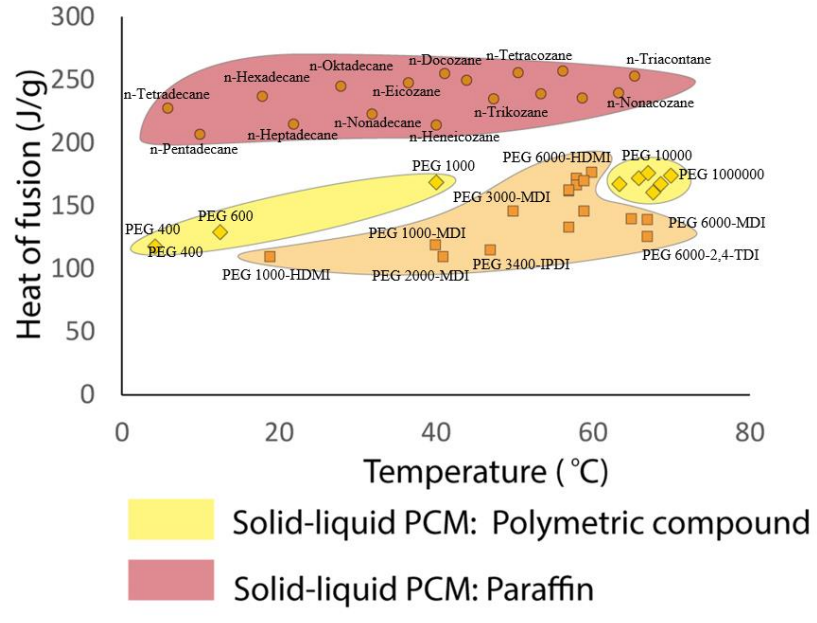


Trade-off between heat capacity and thermal conductivity
Spread heat uniformly, absorbing it at the same time

# Structural Characterization of Ga:PCM Composite

Optical images of Ga:PCM samples, pure PCM (0%) and pure Ga (100%)

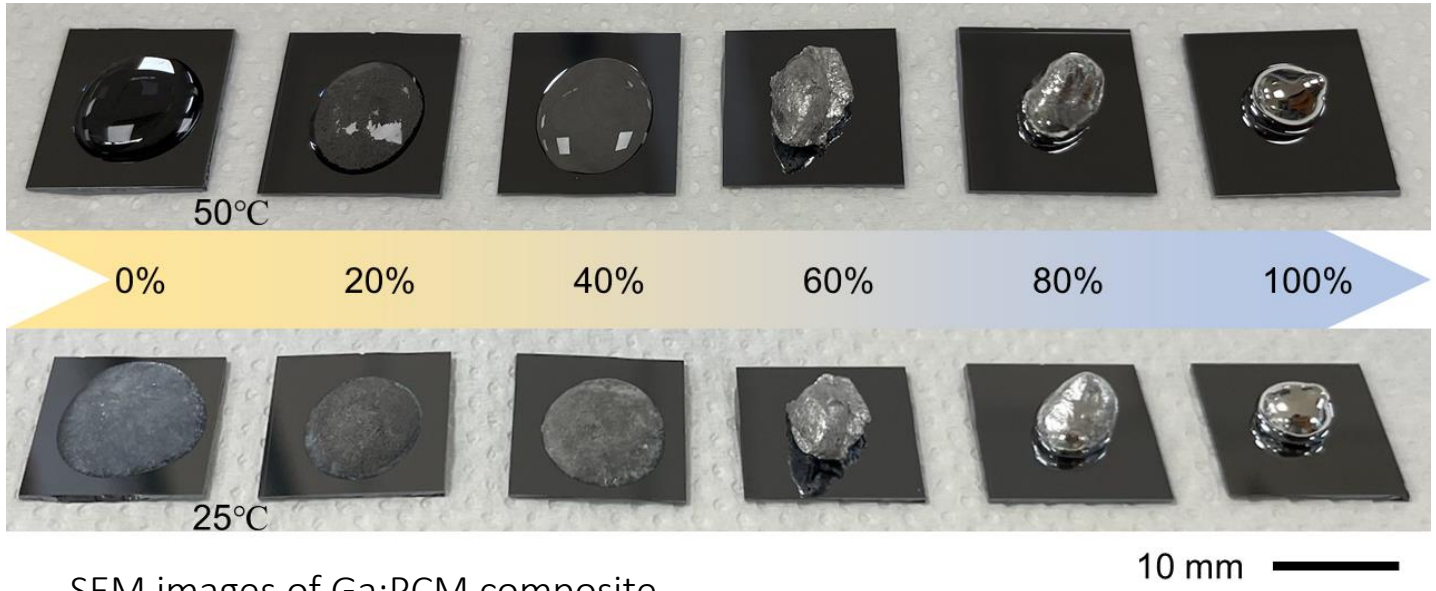


SEM images of Ga:PCM composite

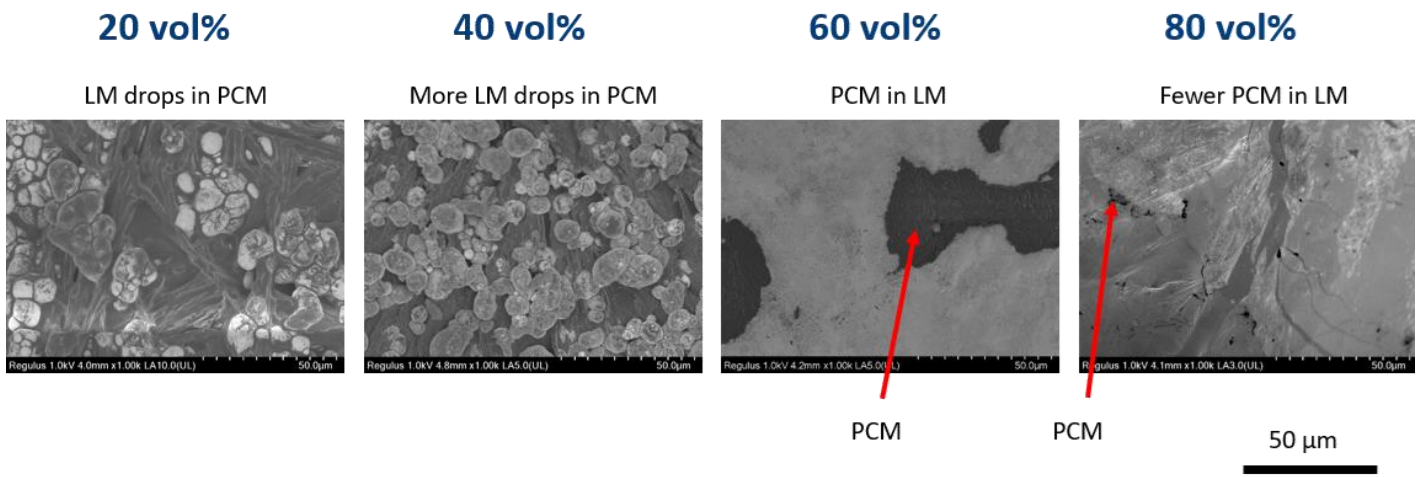


EDX mapping

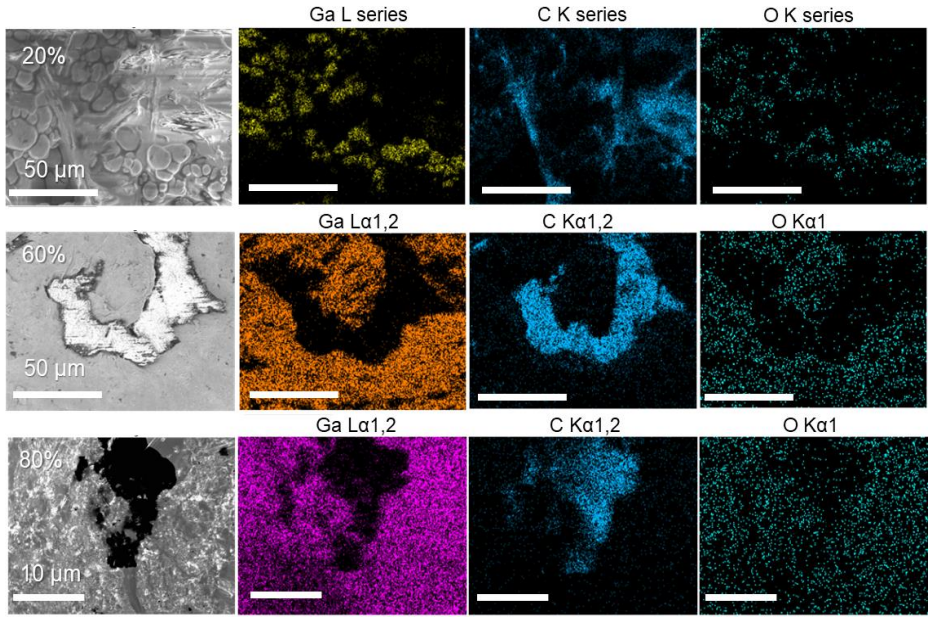


Ga particle sizes ~10 µm

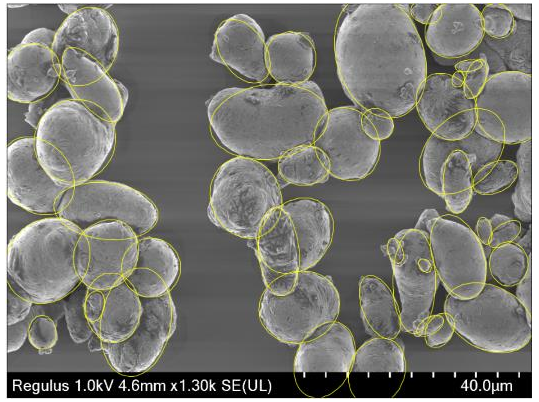


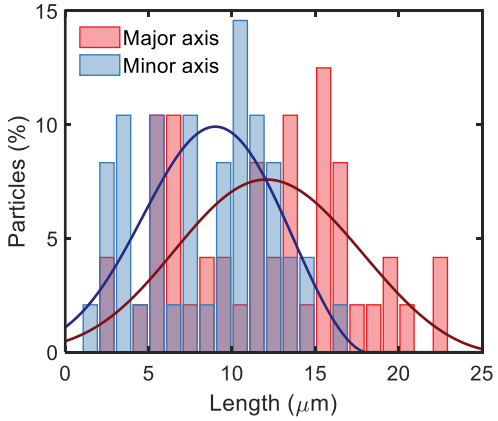

# Thermal Performance of Ga:PCM Composites

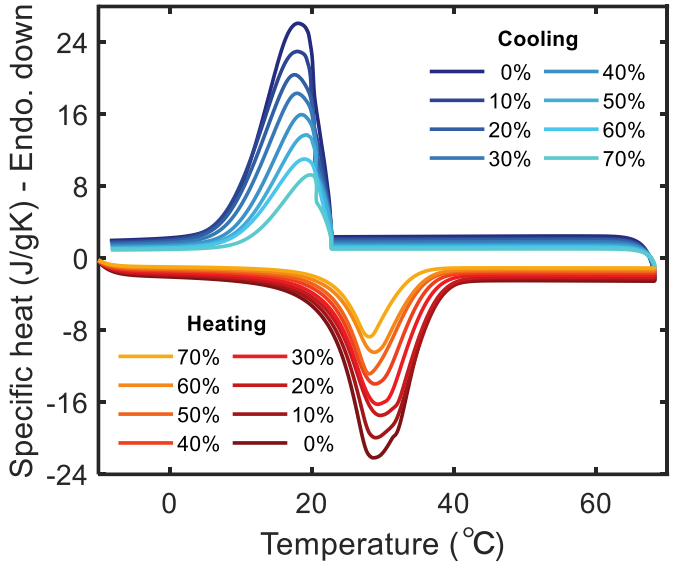


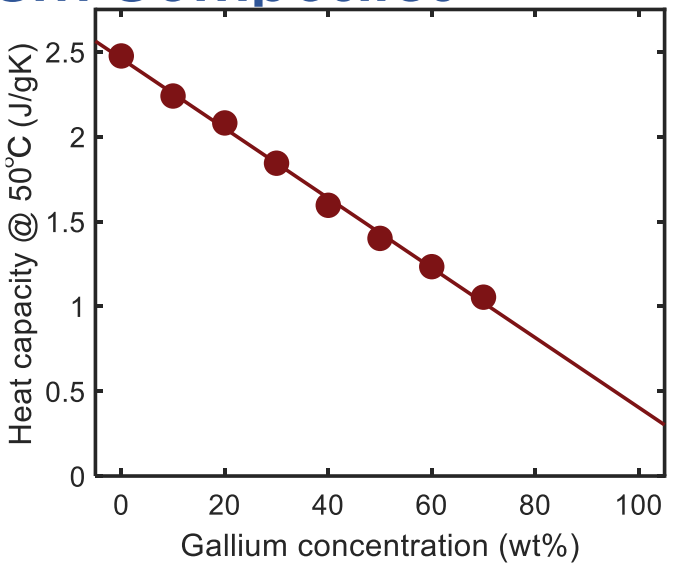


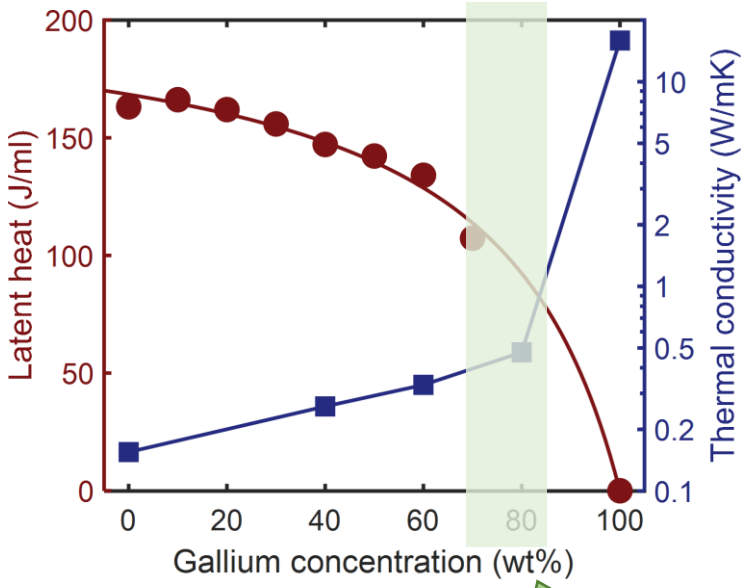


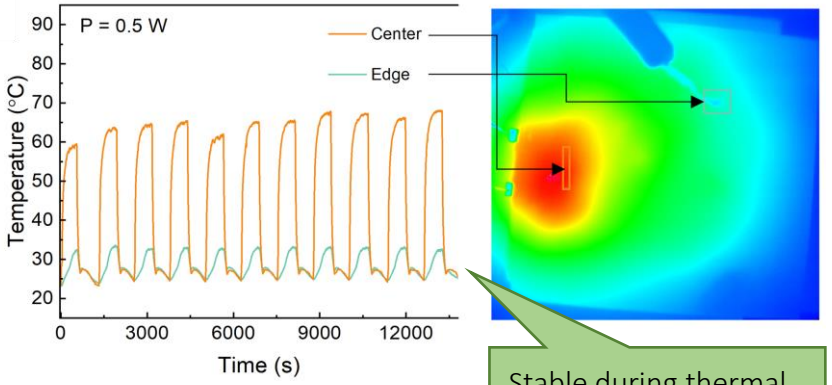


Stable during thermal cycling

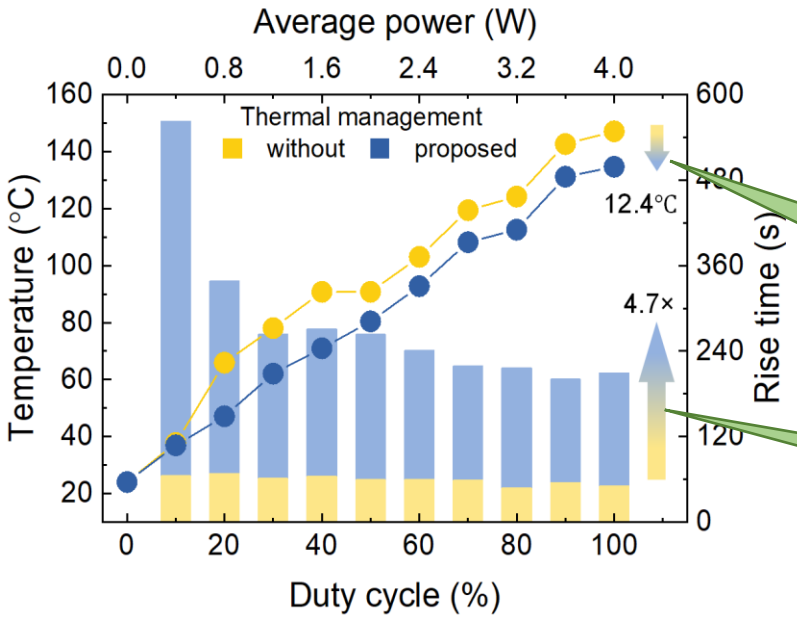


Optimal Ga concentration to achieve the best tradeoff between thermal conductivity and latent heat within the composite material

Average reduction in equilibrium temperature by 12.4℃

Average overheating delay of 4.7 times

# Radiative Cooling Structures Based on Carbon Nanotubes

The Absorption Length, Emissivity, and Specific Heat of a material influence its cooling speed

In radiative cooling, a material with a shorter absorption length can absorb heat from the surroundings effectively and cool down faster

Higher emissivity values indicate that a material emits thermal radiation more efficiently

Materials with lower specific heat can cool down faster once they have absorbed heat

| Material | Absorption Length (μm) | Emissivity | Specific Heat (J/g·K) |
|---|---|---|---|
| **Copper** | ~0.5-2.5 | ~0.03-0.05 | 0.39 |
| **Aluminum** | ~0.5-2.5 | ~0.03-0.05 | 0.90 |
| **Silicon** | ~1.1 | ~0.7 | 0.71 |
| **PDMS** | ~0.2-2.5 | ~0.10-0.15 | 1.70 |
| **n-octadecane** | ~0.5-3.0 | ~0.80-0.95 | 2.10 |
| **Polyimide** | ~2.0-3.0 | ~0.80-0.95 | 1.35 |
| **Carbon Nanotubes** | ~2-10 | ~0.8-0.98 | 0.5-1.5 |
| **Graphene** | ~0.1-1 | ~0.98 | 0.7-0.9 |
| **Graphite** | ~0.1 | ~0.95 | 0.71 |

Carbon based materials have the best properties for radiation-dominated cooling

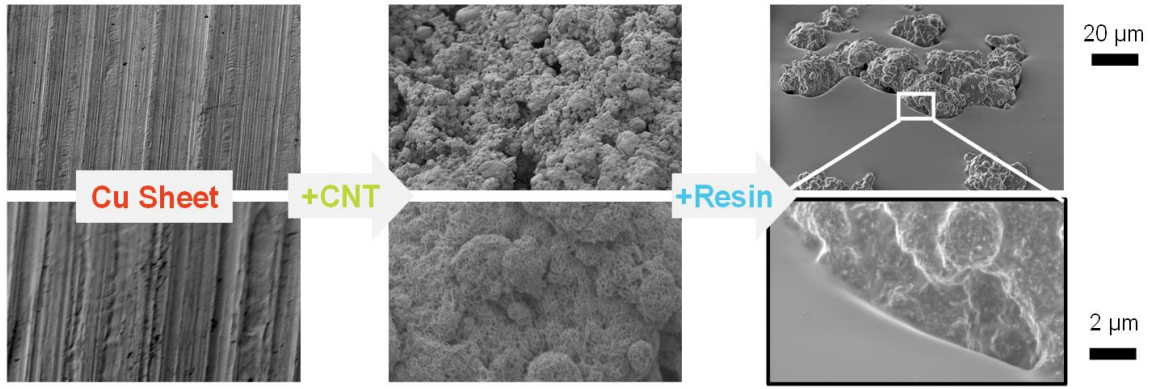


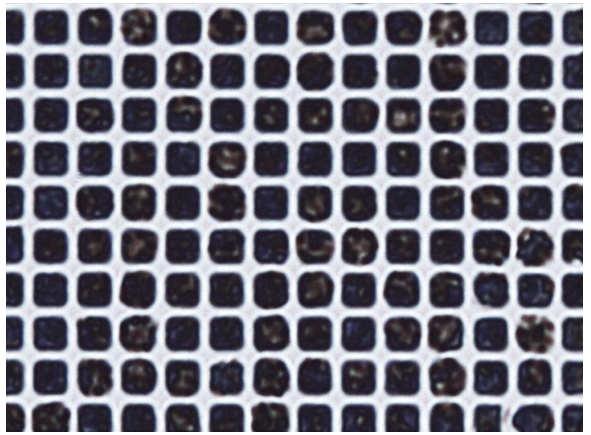

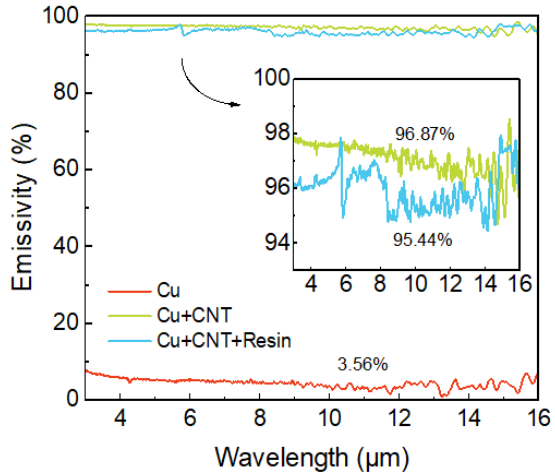

# Demonstrating Combined Effects of Layered Thermal Stack

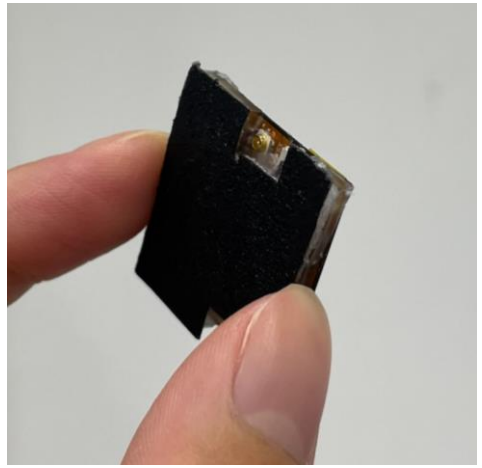

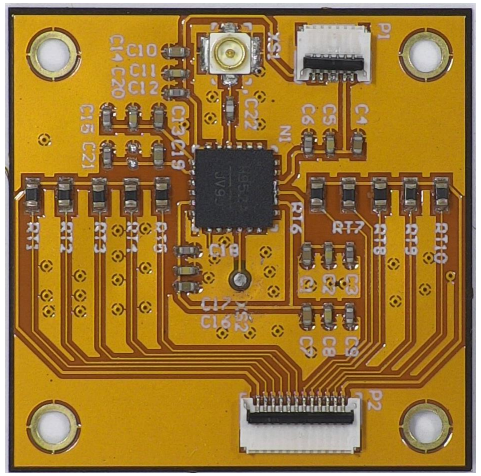

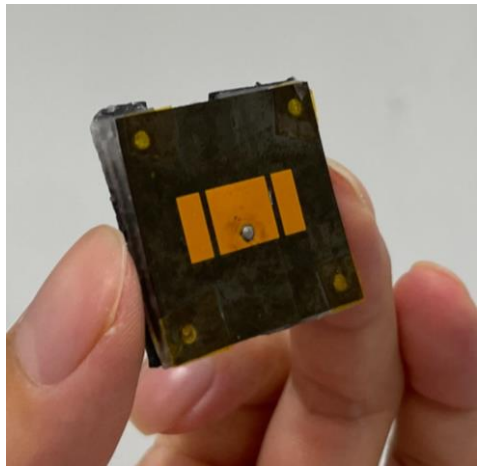

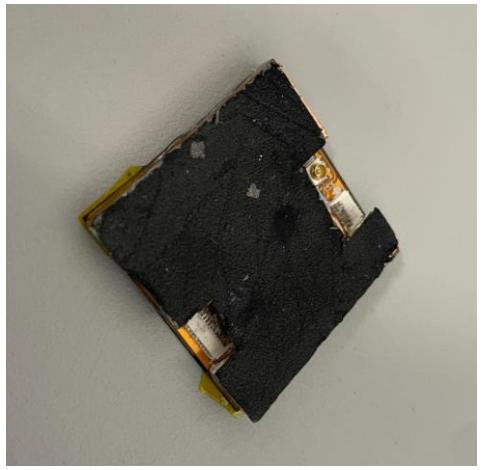

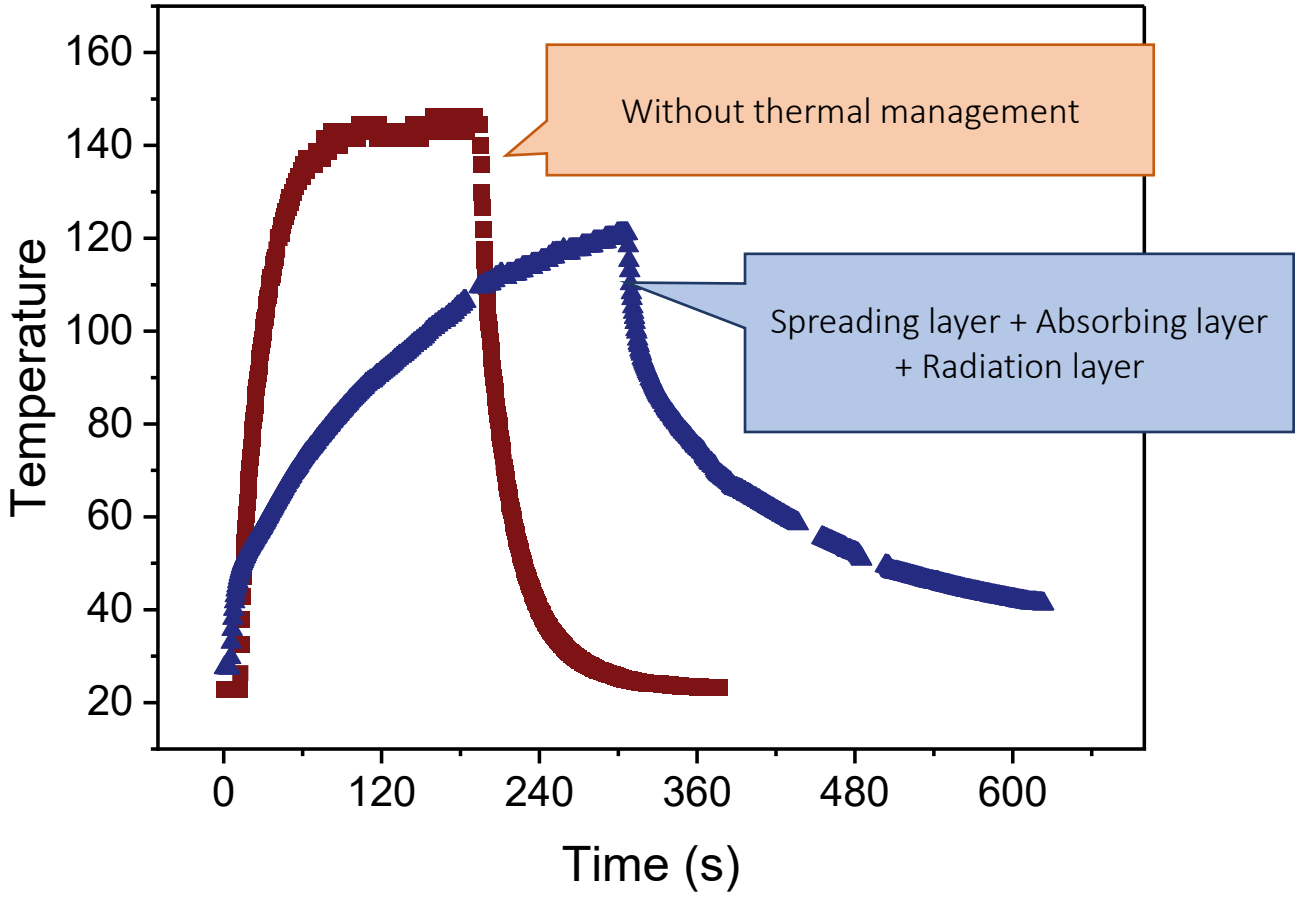

# PCB Level Thermal Management:

# Active Thermal Management Solution

# Proposed Magnetically-Driven PCM Slurry Cooling System

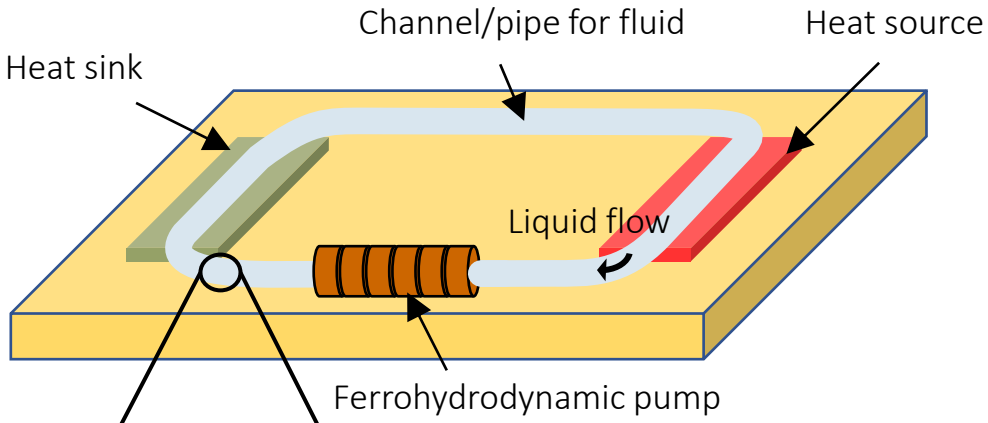


Schematic of the cooling system using MPCM slurry and ferrohydrodynamic pump

Key Features:

- Without mechanical moving part
- Higher heat capacity than water
- Faster than natural convection

Photograph of the slurry

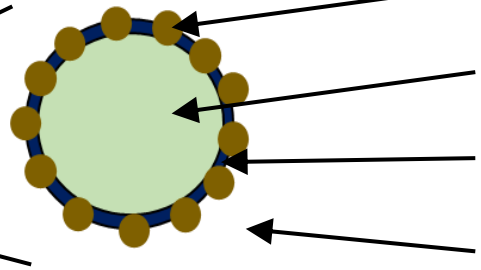

Schematic of the Micro-encapsulated PCM (MPCM)

Magnetic iron oxide nanoparticles (MIONP)

PCM (e.g., n-Octadecane)

Polymer shell (e.g., Melamine formaldehyde (MF))

Water

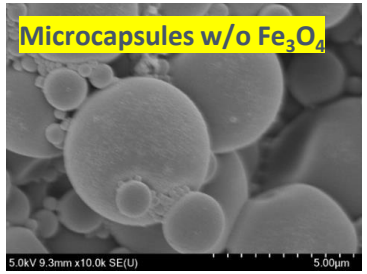


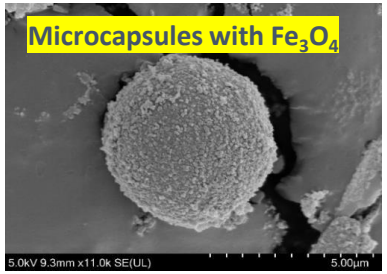

# Thermal and Magnetic Characterization

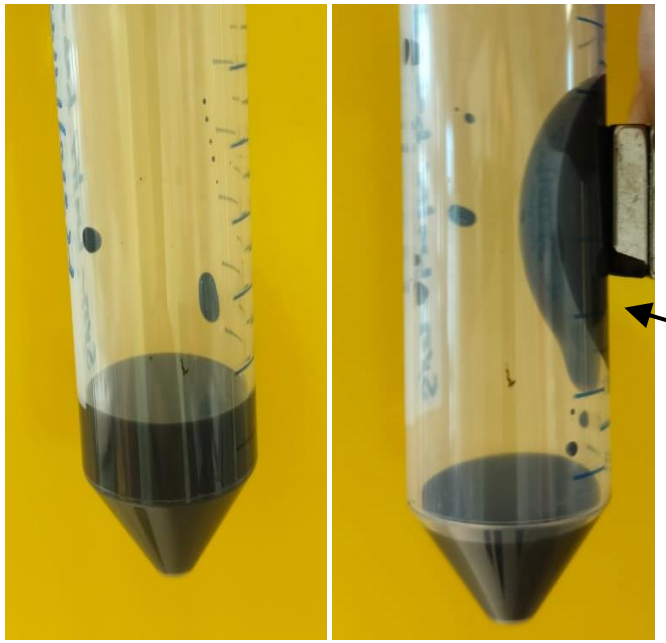


Demonstration of magnetic property of the slurry

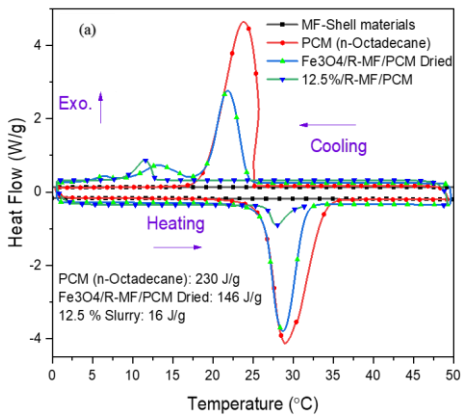


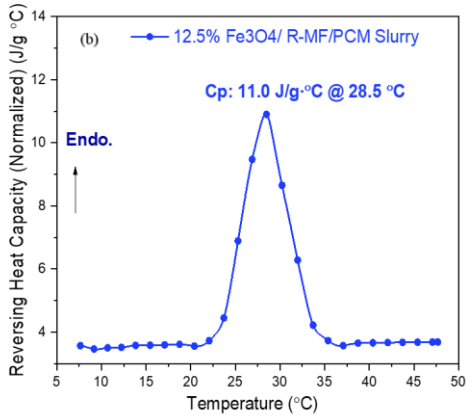


Thermal properties of MPCM and slurry

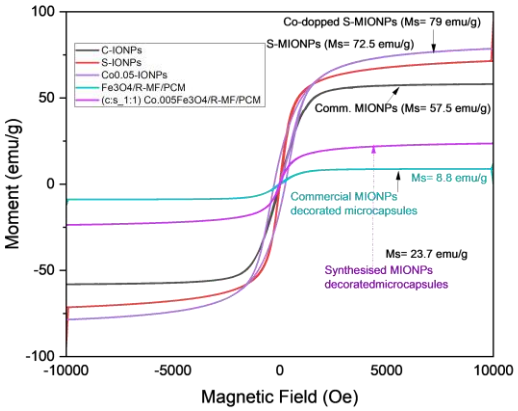


Magnetic properties of MPCM

MPCM Statics:

- Average size ~ 5 µm
- Latent heat = 146 J/g (MPCM), or = 11 J/g (Slurry)
- Magnetic moment = 23.7 emu/g

# Performance Comparison: MPCM Slurry vs. Water Cooling

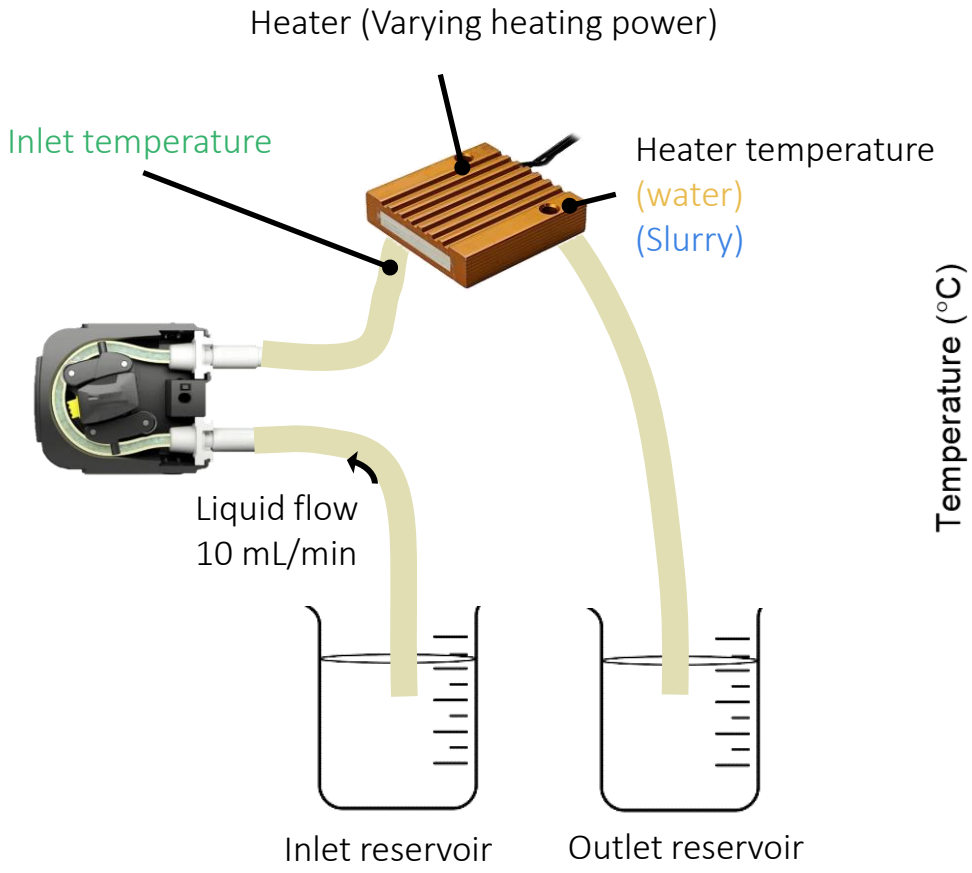


Illustration of experimental setup

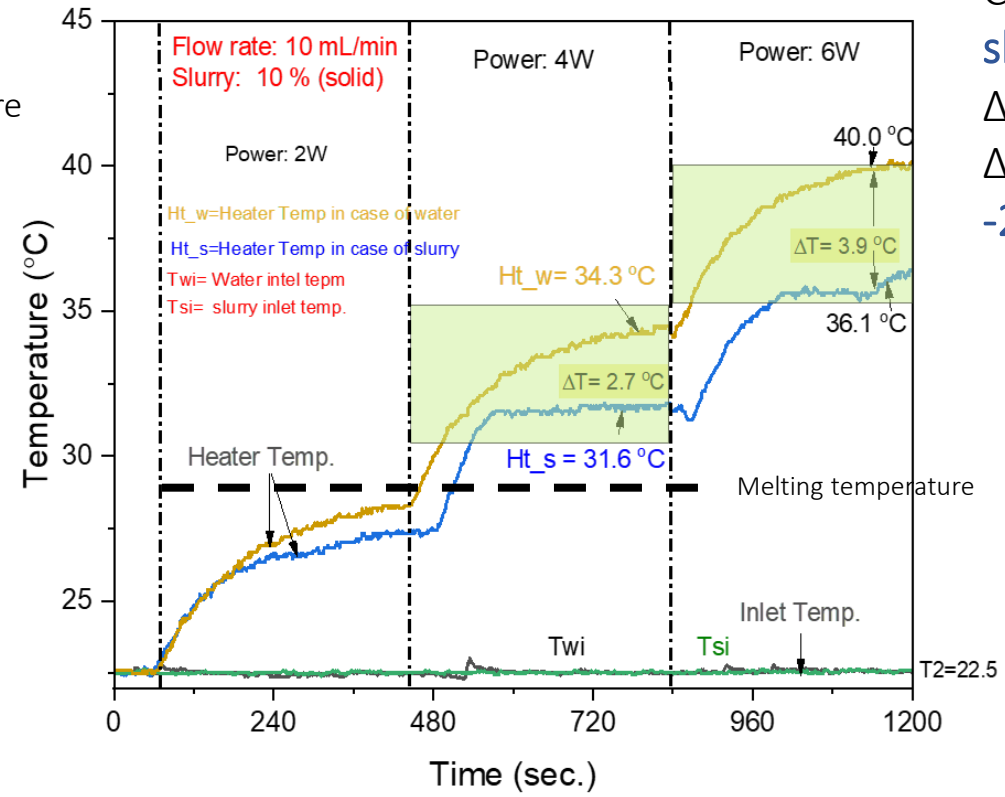


Comparison between MPCM slurry and water in cooling performance

Compared to **water**, our **slurry** achieved:

ΔT = **2.7 ℃** @ 4 W

ΔT = **3.9 ℃** @ 6 W

**-22.6%** in Thermal resistance

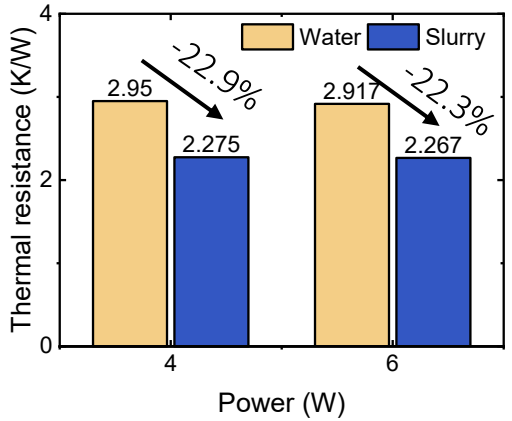


Comparison of thermal resistance

# Ferrohydrodynamic Pumping: Timing and Coil Control

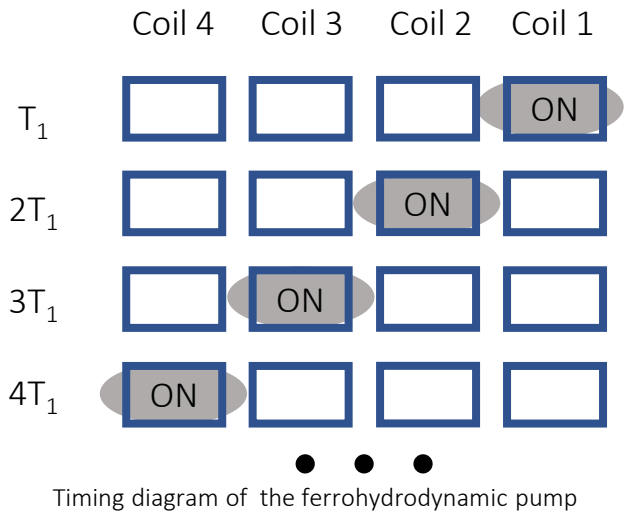


Timing diagram of the ferrohydrodynamic pump

Magnetic body force

$$F = \nabla(M \cdot B)$$

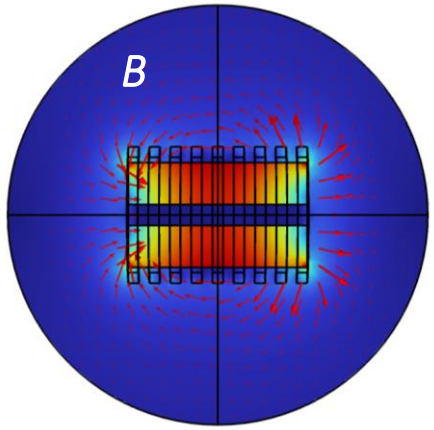


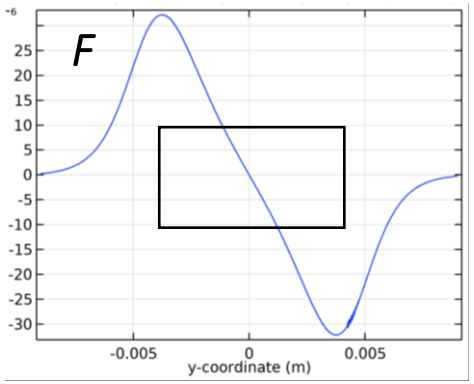


Coils are activated in sequence to realize continuous movement

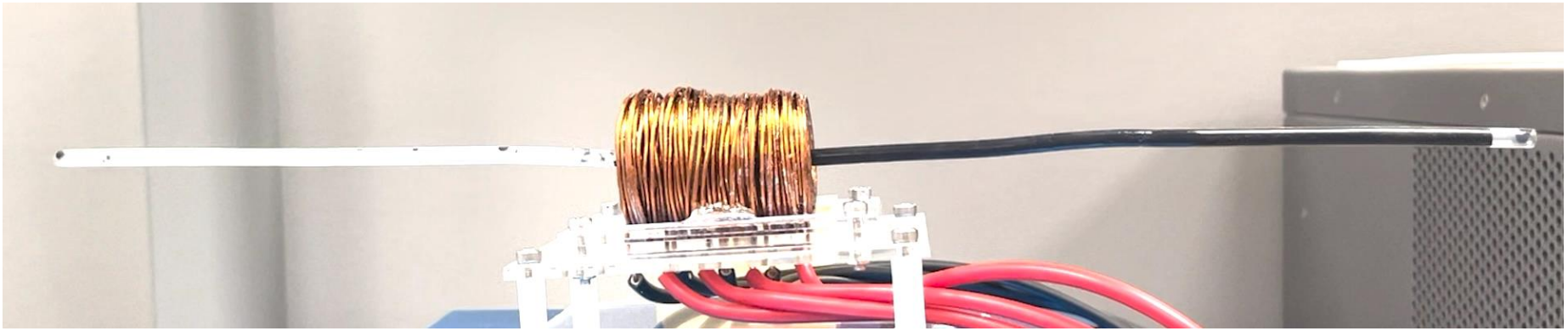

# Summary

- Proposed compact, scalable thermal management solutions compatible with chip, interposer, and board levels, for RF, AI, and high-density electronics.

- Wafer-Level Thermal Management

Developed high-power thermoelectric cooling systems and micro-jet impingement arrays enabling rapid temperature uniformity ($\Delta T < 1$ °C) and high heat flux handling up to 1.25 W/mm².

- Interposer-Level Innovations

Demonstrated the use of SiC substrates and hybrid bonding to lower hot spot temperatures by up to 26%, enabling 22–23% higher component density.

- PCB-Level Passive Thermal Management

Designed layered structures combining heat spreading, adsorption, and radiation using materials like graphite, Ga composites, and CNTs, reducing temperatures and improving uniformity.

- Active Cooling: Magnetic MPCM Slurry

Developed a magnetically driven slurry cooling system using microencapsulated PCMs and ferrohydrodynamic pump. Achieved a 22.6% reduction in thermal resistance over water cooling without mechanical pumps.

# Thank You